İSTANBUL TECHNICAL UNIVERSITY ★ INSTITUTE OF SCIENCE AND TECHNOLOGY

ROLL FORMING OF BIFURCATED PROFILES

M.Sc. Thesis by
Mehmet Okan GÖRTAN, B.Sc.
(503051208)

Date of submission : **5 May 2008**

Date of defence examination: **11 June 2008**

Supervisor (Chairman): **Assoc. Prof. Dr. Haydar LİVATYALI**

Members of the Examining Committee **Prof.Dr. Mehmet DEMİRKOL**

Assoc. Prof. Dr. Hikmet KOCABAŞ

JUNE 2008

<u>İSTANBUL TEKNİK ÜNİVERSİTESİ ★ FEN BİLİMLERİ ENSTİTÜSÜ</u>

AYRILMIŞ PROFİLLERİN MAKARALI BÜKÜLMESİ

YÜKSEK LİSANS TEZİ

Müh. Mehmet Okan GÖRTAN
(503051208)

Tezin Enstitüye Verildiği Tarih : 5 Mayıs 2008
Tezin Savunulduğu Tarih : 11 Haziran 2008

Tez Danışmanı : **Doç.Dr. Haydar LİVATYALI**

Diğer Jüri Üyeleri **Prof.Dr. Mehmet DEMİRKOL**

Doç. Dr. Hikmet KOCABAŞ

HAZİRAN 2008

ACKNOWLEDGEMENTS

First of all, I would like to thank my university advisor Assoc. Prof. Haydar Livatyalı for encouraging me to make my master studies abroad.

Secondly, I would like to express my gratitude to Prof. Dr.-Ing.Dipl.-Wirtsch.-Ing. Peter Groche for giving me the opportunity to make my master studies at PtU at TU Darmstadt. I also want to thank Dipl.-Ing. Dragoslav Vucic, my advisor at PtU, for his wise guidance and support throughout this research.

Finally, I would like to thank my family for their encouragement, patience and endless support.

JUNE 2008 Mehmet Okan Görtan

TABLE OF CONTENTS

ABBREVIATIONS

BC	: Boundary Condition
CAE	: Computer Aided Engineering
DCS	: Deformed Curved Surface
DIN	: German Institute for Standardization
FE	: Finite Element
FEM	: Finite Element Method
FL	: Flange Length
PtU	: Produktionstechnik und Umfommaschinen
SFB666	: Special Research Field 666
TU	: Technical University
WH	: Web Height

LIST OF TABLES

Page No.

LIST OF FIGURES

Page No.

LIST OF SYMBOLS

θ	: Bending angle
φ	: Logarithmic strain
ε	: Strain
$\Delta\varepsilon_{max}$	: Maximum strain difference
ΔX	: Distance of the maximum strain point to the station surface
σ_y	: Yield strength
K	: Strength index
k_θ	: Bending angle correction factor
k_f	: Flange length correction factor
k_s	: Web height correction factor
L	: Deformation length
L*	: Length of the deformed edge of the strip
l_f	: Flange length
l_s	: Web height
n	: Shape function parameter
n	: Strain hardening index
s	: Circular path of the flange edge point
S(x)	: Shape function
s_h	: Hinge height
t	: Sheet thickness
W_B	: Plastic work done per unit length
$W_{B,L}$	: Plastic work done per unit length of the hinge
$W_{B,V}$	: Plastic work done per unit volume
W_t	: Total work
x	: Coordinate in longitudinal direction
y	: Coordinate in transversal direction
z	: Coordinate in thickness direction

AYRILMIŞ PROFİLLERİN MAKARALI BÜKÜLMESİ

ÖZET

Makaralı bükme, yüksek esnekliği ve verimliliği nedeniyle karşımıza en önemli imalat yöntemlerinden biri olarak çıkmaktadır. Bu yöntem ile şekil, malzeme, kalınlık vb. açısından birbirinden ayrılan birçok profilin imal edilmesi mümkündür. Yeni bir imalat yöntemi olan lineer akışlı ayırma, makaralı bükmede kullanılan yarı mamullerin çeşitliliğini artırmıştır. Ayrılmış profillerin makaralı bükmede kullanılmasıyla bu imalat yönteminin ürün gamı genişletilebilir.

Ayrılmış profillerin makaralı bükülmesi sırasında oluşan analitik ilişkilerin tanımlanması bu çalışmanın temelini oluşturmaktadır. İncelemelerin merkezinde de ayrılmış profillerin makaralı bükülmesi sırasında oluşan boylamasına birim şekil değişimi bulunmaktadır. Çalışmalar sırasında sonlu elemanlar yöntemi kullanılmıştır. Kanat yüksekliği, kanatçık uzunluğu ve bükme açısı gibi değişkenler daha önceden belirlenmiş adımlar halinde değiştirilmiştir. Makaralı bükme sırasında boylamasına yönde oluşan maksimum birim şekil değişimi incelenmiştir.

Yapılan sonlu eleman analizlerinin sonuçları kullanılarak ayrılmış profillerin makaralı bükülmesi sırasında oluşan boylamasına birim şekil değişimleri üzerine genel değerlendirmeler yapılabilir. Boylamasına birim şekil değişimi değerlerinin kanat yüksekliğine bağlı olarak bir minimum değeri vardır. Kanat yüksekliğinin bu seviyenin altına indirilmesi veya üzerine çıkarılması birim şekil değişimi değerlerinin artmasına neden olur. Bükme açısının düşürülmesinin boylamasına birim şekil değişimi değerleri üzerine olumlu etkisi vardır, yani bükme açası azalırken boylamasına birim şekil değişimi değerleri de azalır. Buna karşın, kanatçık uzunluğu artarken birim şekil değişimi değerleri azalır. Lineer yaklaşım kullanılarak ayrılmış profillerin makaralı bükülmesi sırasında kanat yüksekliği, kanatçık uzunluğu ve bükme açısına bağlı olarak oluşan maksimum boylamasına birim şekil değişiminin hesaplanması için bir formül tanımlanmıştır.

ROLL FORMING OF BIFURCATED PROFILES

SUMMARY

Because of its high flexibility and productivity, roll forming has developed as one of the most important forming methods. With this method, many profiles varying in their shape, materials, thickness, etc. can be produced. The new production method, linear flow splitting enlarges the range of the semi finished products which can be used in roll forming. With the utilization of the splitted profiles in roll forming, the product spectrum of this forming method can be enlarged.

The definition of the analytical relations during roll forming of bifurcated profiles creates the basis of this study. The longitudinal strain occurring during roll forming of the bifurcated profiles is the center of the investigations. During the studies, an FE approach will be implemented. The parameters such as web height, flange length and bending angle will be varied in predefined steps. The maximum strain occurring during roll forming in longitudinal direction will be analyzed.

Evaluating the results of the finite element simulations conducted, general statements about the longitudinal strain development during roll forming of bifurcated profiles can be made. The longitudinal strain values have a minimum depending on the web height. The reduction of the web height under this level or the increase of it above this level causes an increase in the strain values. The reduction of the bending angle has a positive effect on the longitudinal strain values, namely the strain values decreases as the bending angle decreases. On the contrary, the strain values decrease while the flange length increases. An analytical formula has been defined by using the linear approach to calculate the maximum longitudinal strain occurring during roll forming of the bifurcated profiles depending on the web height, flange length and bending angle.

1. INTRODUCTION

The 90's brought a new word "Globalization" into our vocabulary. In this decade, also the companies have started to feel its influence severely. They created new markets, literally the whole world, for their goods, but in the mean time, they had to compete with other firms from all around the world. This was the case not only for the big companies, also for middle and small sized ones.

The situation was not different for the roll-formers, which are mostly middle and small size companies. These companies had to lower the prices without letting the quality of their products to decrease or come up with new ideas of products or production methods in order to preserve their strength in the global market.

On the other hand, concerns about the environment made governments take precautions especially about global warming. One of these precautions is the reduction of the exhaust gases of the motor vehicles, particularly CO_x and NO_x. This increased the demand on lightweight vehicle structures.

Because of the pressure of the global market on one side and the demand on lightweight structures on the other side, the necessity of new production concepts has arisen. As a response to this problematic, a new massive forming method "linear flow splitting" has been developed at Institute for Manufacturing Techniques and Forming Machines (PtU) at TU Darmstadt. With this production method, the generation of the integral bifurcations in sheet metal has become possible without material doublings.

2. STATE OF THE ART

2.1 Conventional Roll Forming

2.1.1 Classification and definition of roll forming

According to DIN 8582, forming techniques are divided into five subgroups depending on the main direction of the applied stress [1]. One of the subgroups is the forming by bending (Fig. 2.1).

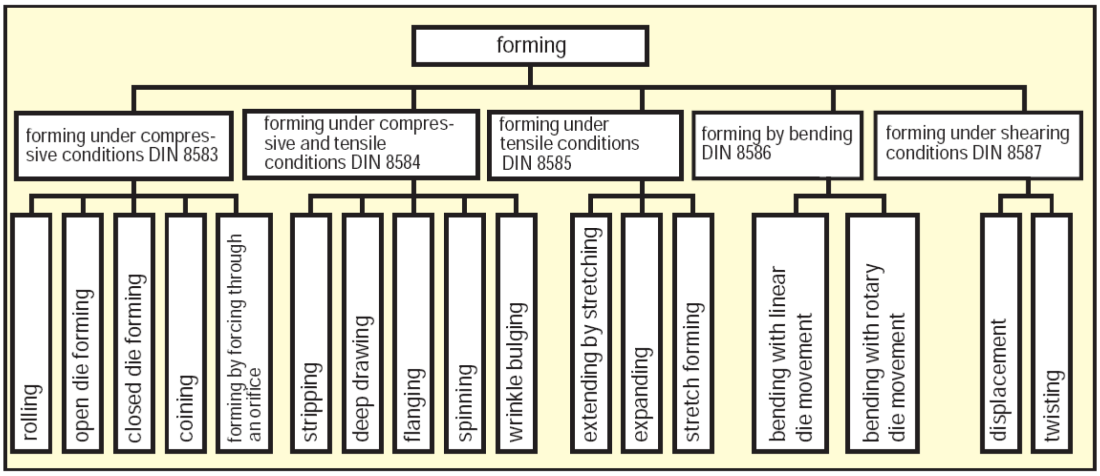

Figure 2.1: Classification of the Forming Techniques used in Forming [2]

According to DIN 8586, roll forming is a forming technique with rotary die movement [3]. It is defined as a forming method, where the sheet metal strip is formed along straight, longitudinal, parallel bend lines with multiple pairs of countered rolls without changing the thickness off the material at room temperature. However, this definition has also exceptions. The product may have curved or spiral form, it may have bend lines 90^0 to the longitudinal bend line; by the roll forming line, bronze shoes or plastic guides may be used in addition to countered rolls; the thickness is almost always reduced at the bend lines and the strip material may be heated up to a certain temperature or the material may be hot roll formed [4].

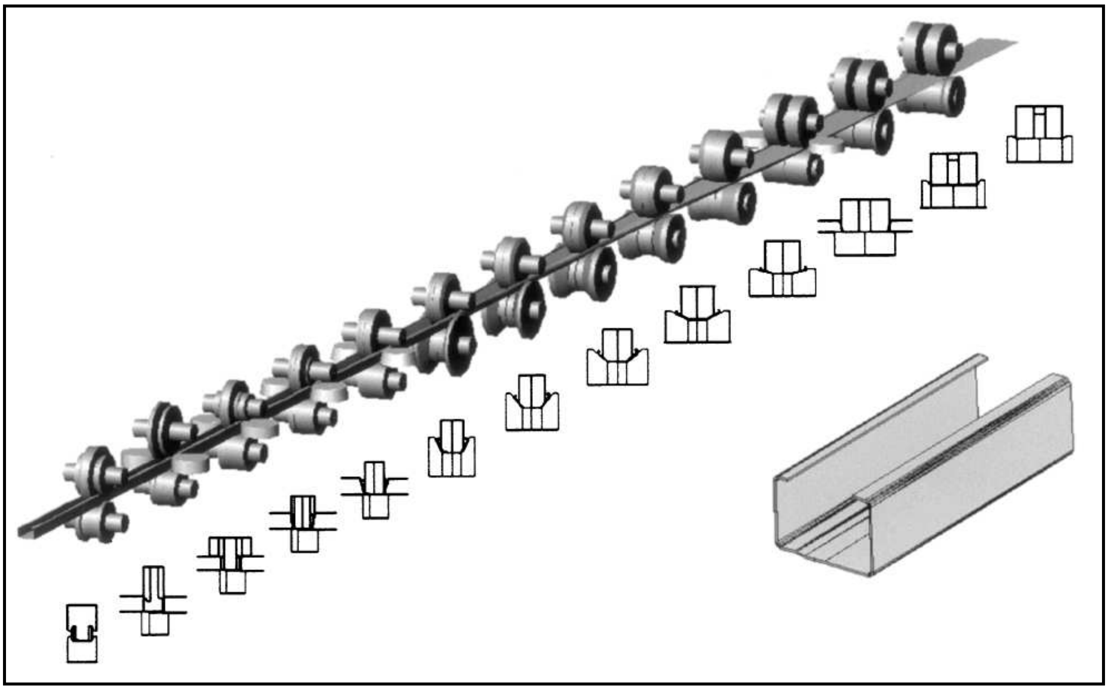

Figure 2.2: Schematic Representation of the Roll Forming Process [4]

Roll forming is one of the most productive metal forming technologies. About 35 to 45 % of all flat steel produced by the North American steel mills is processed through roll forming mills [4]. A wide range of products spreading from medical equipment to car body parts is manufactured using this working method. It allows production of many beams with different cross sections from strips with varying of lengths and thicknesses that variate from 0.2 mm to 20 mm with a production velocity of up to 200 m/min [5, 4].

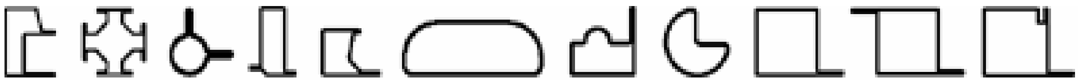

Figure 2.3: Different Roll Formed Closed Beams and Profiles [6]

Roll forming lines are divided into two groups based on their operating modes; start-stop lines and continuous running lines. Start-stop lines are made in their simplest form of a decoiler, a coil loop, a roll forming machine and a parting die. By this method cut-to-length blank metal sheets are processed. The product length is defined by the roll forming machine. Operations like blanking and embossing are also possible by start-stop lines using the roll forming machine's positioning system.

Contrary to start-stop lines, continuous running roll forming lines operate at a constant speed. They are advantageous while processing sheet metal blanks or strips to create long sections. The produced profiles are parted after roll forming using automatic cut-to-length devices.

One of the advantages of a blank processing line (start-stop line) is the possibility to use a simple cross-cutting shear instead of a complex profile parting die. This prevents the additional cost of the die inserts. However, by start-stop lines, only sheet metals with a certain minimum length can be processed, because the feed force acting on the sheet metal has to be greater than the torque necessary for the forming process. Moreover, appropriate guidance tools have to be present in the line in order to support the sheet metal during forming.

The advantage of continuously operating lines is its higher output when processing greater profile lengths. This production method is advantageous if continuously running processes such as longitudinal seam welding, gluing, foaming, etc. are integrated into the roll forming line [2].

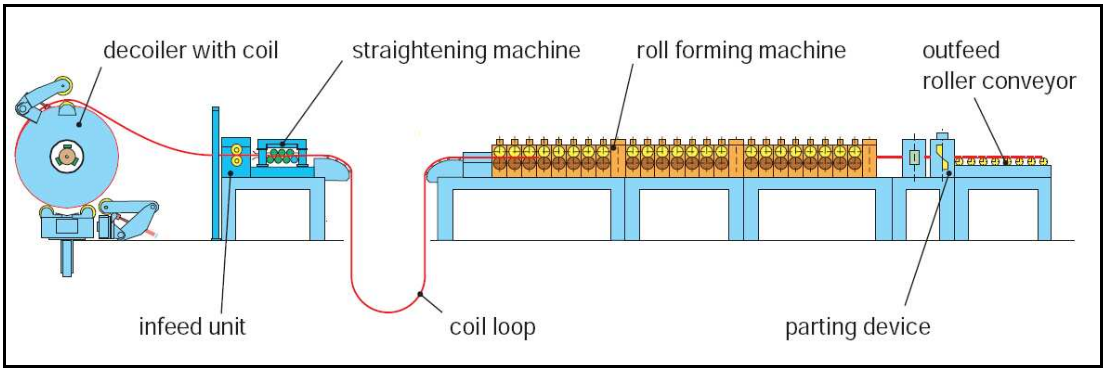

Figure 2.4: Schematic Representation of the Roll Forming Line [2]

2.1.2 Characterization of the deformation in roll forming

In roll forming processes, metal strips are subject to various types of deformations. These deformations may be divided into two categories; transversal bending and redundant deformations [4].

2.1.2.1 Transversal bending

The most important and actually desired deformation in roll forming for metal strips is transversal bending deformation. Transversal bending is needed to form metal strips into products with required cross-sections (Fig. 2.5). Gradual forming is achieved by using a series of contoured rolls [4].

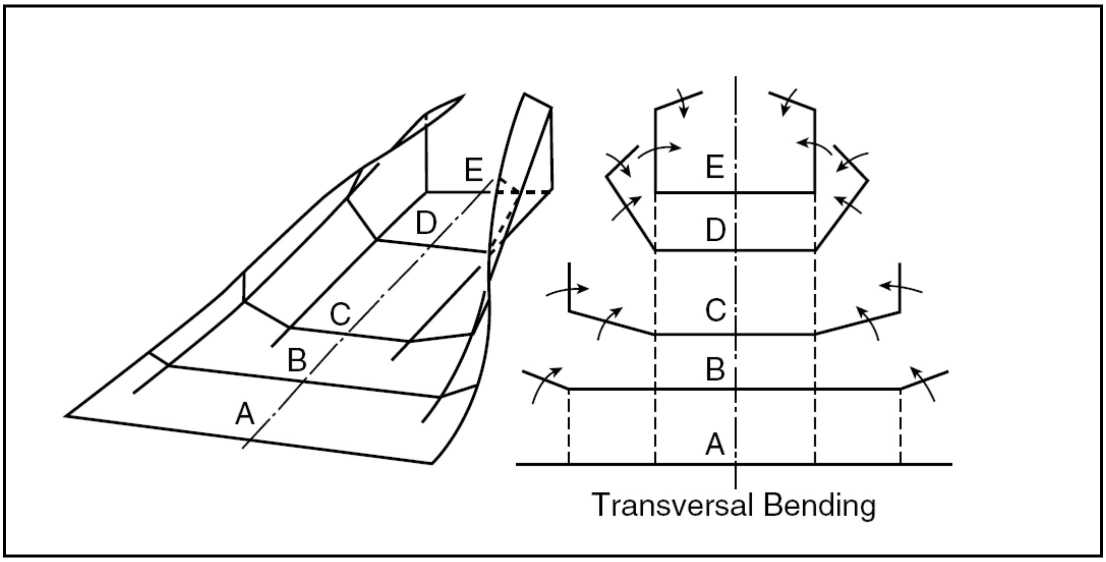

Figure 2.5: Schematic Representation of the Transversal Bending during Roll Forming [4]

2.1.2.2 Redundant deformations

During roll forming, metal strips are subjected to many other deformations in addition to transversal bending. Metal strips are entered into roll forming mills either in precut or coil form and are gradually deformed into complicated three-dimensional shapes by a series of contoured rolls before they are finally made into products. Because of this process, various types of additive redundant deformations are induced in the metal (Fig. 2.6) [4].

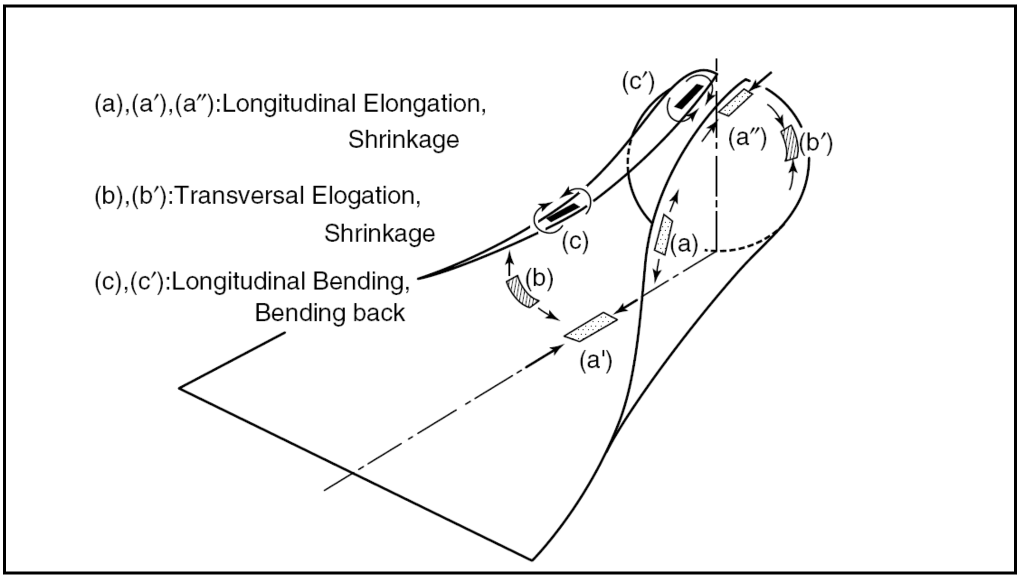

Figure 2.6: Redundant Deformations of the Metal Strip during Roll Forming [4]

These redundant deformations are superimposed on the transversal bending and they significantly influence the formation of the product's cross-section and shape. Many problems, which occur in roll forming processes, are related to redundant deformations [4].

The redundant deformations are mainly investigated in three groups:

1. Longitudinal elongation or shrinkage
2. Transversal elongation and shear in strip's plane
3. Longitudinal bending and bending back

In roll forming processes, strips are successively bent in the transversal direction and their cross-sectional profile is incrementally transformed to the desired form. During this forming process, edge portions of the strip usually move along flow lines which are longer than those of the center portions (Fig. 2.7). This is the main reason of the longitudinal elongation or shrinkage [4]. The longitudinal elongation is the main criterion to design the flower diagram by roll forming [7].

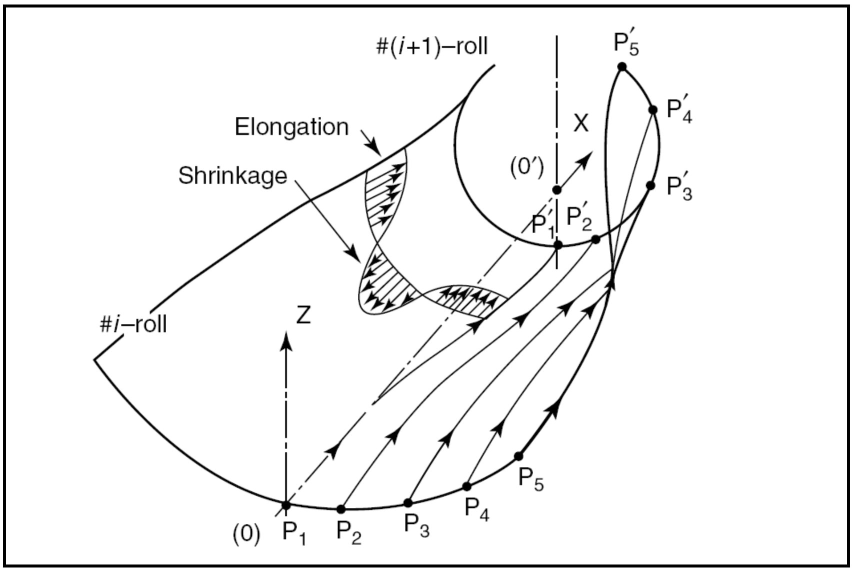

Figure 2.7: Mechanism of Occurrence of Longitudinal Elongation and Shrinkage of Metal Strip [4]

During the production of the wide cross sections via roll forming, quite a large force is required to pull the edge and the intermediate portions of the sheet metal. Because of this transversal force, transversal elongation occurs in the sheet metal.

As sheet metals are formed in a roll forming line, each portion of the metal strip is bent in the longitudinal direction in between two consecutive forming stations and they are bent back as they reach the center of the roll gap. This repeated longitudinal forward and back bending is especially extensive at the edge portion of the strip. The repeated longitudinal bending and bending back under the longitudinal tensile stress contributes to the longitudinal elongation [4].

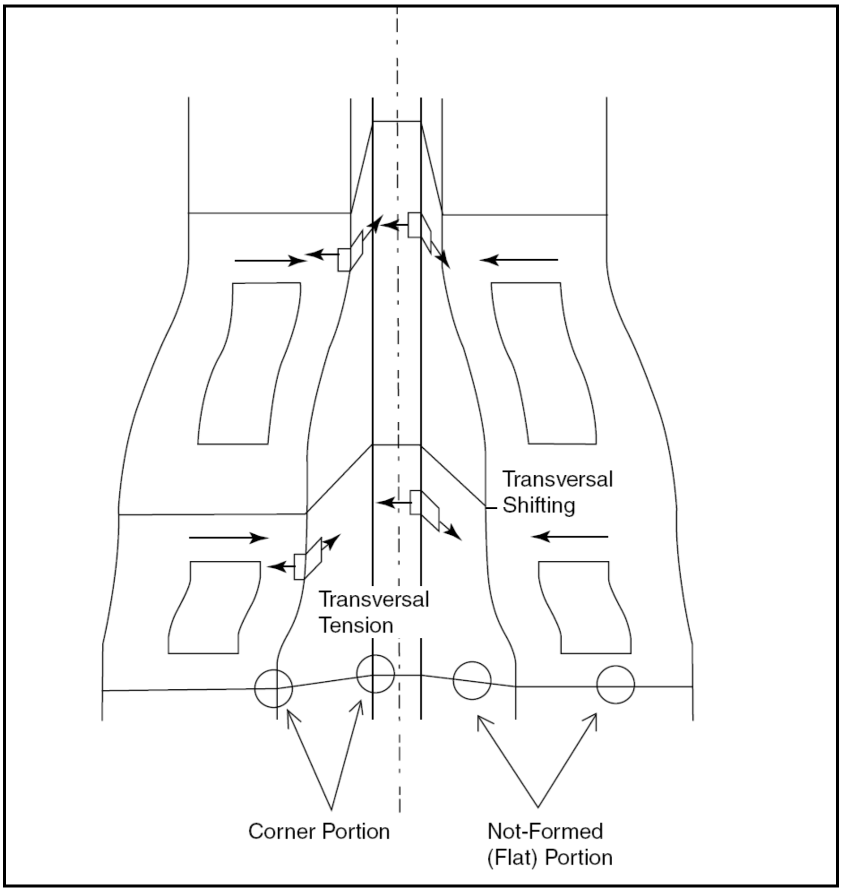

Figure 2.8: Mechanism of Generation of the Transversal Forces acting to Metal Strip [4]

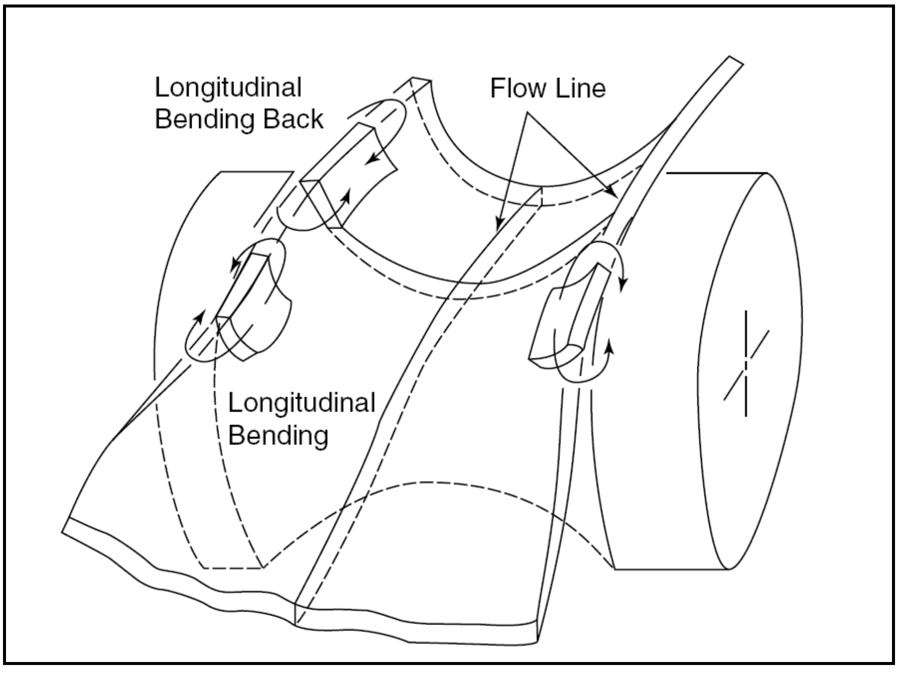

Figure 2.9: Mechanism of Occurrence of Longitudinal Bending of Metal Strip [4]

2.1.2.3 Effects of the redundant deformations

The redundant deformations affect the transversal bending of the strip which is necessary to achieve the desired shape of the product. They also influence stresses and strains induced in metal strips during roll forming, springback deformations after forming, and the distribution of residual stresses in the products.

In other words, the redundant deformations cause a variety of defects in the roll formed products. Longitudinal bow, camber or twist, edge wave, center (or pocket) wave, herringbone effect, thinning, cracking, splitting, flare (distortion of cutoff end), and dimensional inaccuracy are some examples of these defects [4].

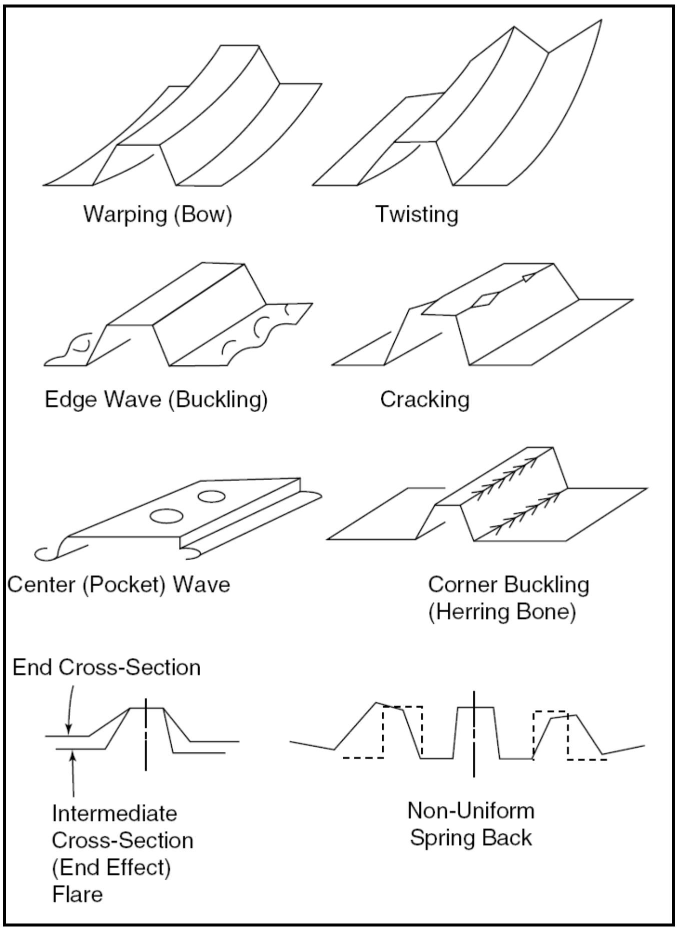

Figure 2.10: Schematic Illustrations of Defects of Products [4]

2.1.3 Mathematical modeling of the forming zone

Bhattacharyya has defined the deformation length in roll forming using a U-profile as basis by minimizing the energy required for bending and stretching in a roll station (Fig.2.11). With this definition, determination of the minimum length in between two roll stations is possible [8].

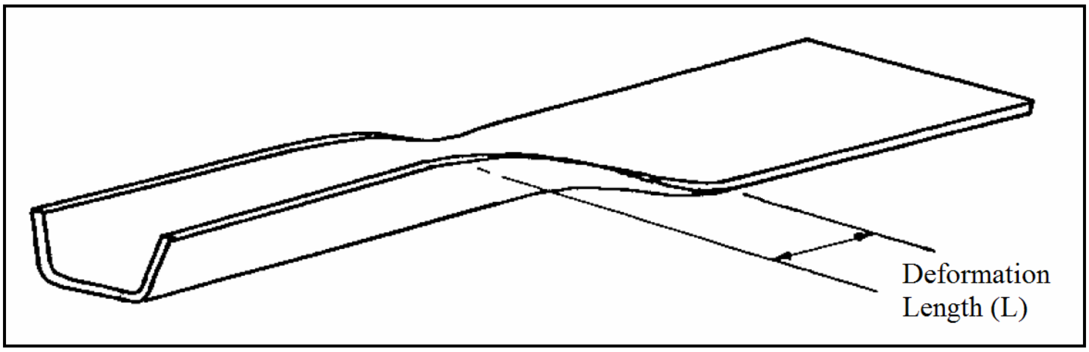

Figure 2.11: Schematic Representation of the Deformation Length [8]

Following assumptions underlie this definition:

- The material is rigid-perfectly plastic,
- Bending takes place only along the folding line,
- The out-of-plane bending of the flange and the longitudinal bending of the web can be neglected,
- The flange takes the shape which minimizes the plastic work [8].

Following figure shows the forming zone and the geometrical values used to determine the length of the deformation length schematically.

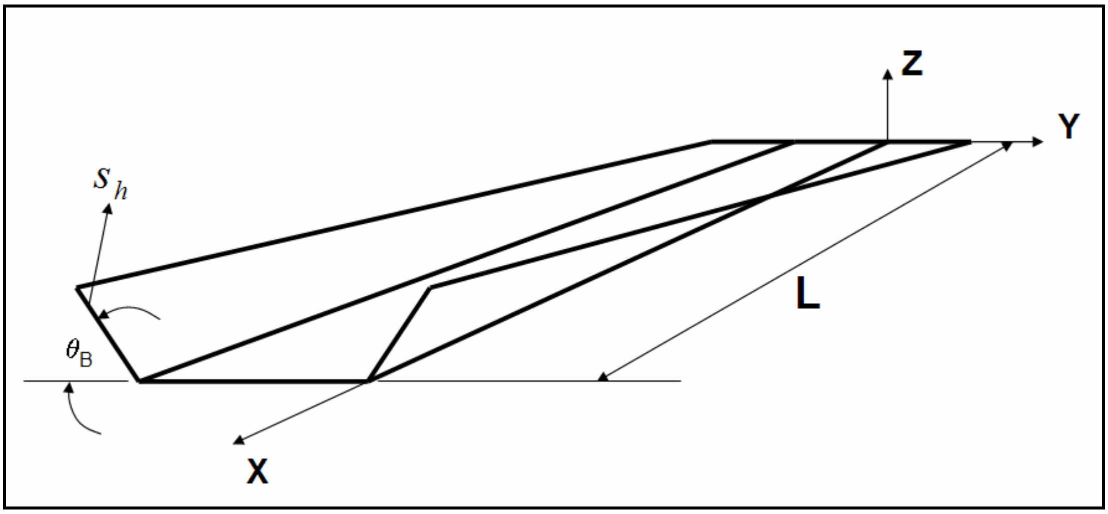

Figure 2.12: Schematic Representation of the Geometrical Values [8]

The plastic work done per unit length of one bend as sheet metal is bent through an angle of θ is

$$W_B = \frac{1}{4}\sigma_y t^2 \theta \qquad \textbf{(2.1)}$$

where σ_y is the yield strength of the used material and t is the thickness of the sheet metal. The plastic work per unit volume is given by

$$W_{B,V} = \frac{1}{2}\sigma_y y^2 \left(\frac{d\theta}{dx}\right) \quad \textbf{(2.2)}$$

Here, y is the coordinate in transversal direction and x is the coordinate in longitudinal direction. With the equation above, the plastic work per unit length of the hinge is

$$W_{B,L} = \int_0^{s_h} \frac{1}{2}\sigma_y y^2 \left(\frac{d\theta}{dx}\right)^2 (tdx) = \frac{1}{6}\sigma_y {s_h}^3 t \left(\frac{d\theta}{dx}\right)^2 \quad \textbf{(2.3)}$$

where s_h is the height of the hinge. Combination of the equations (2.1) and (2.3) gives the plastic work done per unit length

$$W_t = W_B + W_{B;L} = \frac{1}{4}\sigma_y t^2 \theta + \frac{1}{6}\sigma_y {s_h}^3 t \left(\frac{d\theta}{dx}\right)^2 \quad \textbf{(2.4)}$$

Therefore, the total work done for one bend through an angle θ_B is

$$W_t = \int_0^L \left[\frac{1}{4}\sigma_y t^2 \theta + \frac{1}{6}\sigma_y {s_h}^3 t \left(\frac{d\theta}{dx}\right)^2\right] dx = \sigma_y t \int_0^L \left[\frac{t\theta_B}{4} + \frac{{s_h}^3}{6}\left(\frac{d\theta}{dx}\right)^2\right] dx \quad \textbf{(2.5)}$$

The function for the bending angle θ_B which minimizes this expression for the total work satisfies the Euler equation

$$\frac{\partial F}{\partial \theta_B} - \frac{d}{dx}\left(\frac{\partial F}{\partial \theta_B{}'}\right) \equiv \frac{d^2\theta}{dx^2} - \frac{3t}{4{s_h}^3} = 0 \quad \textbf{(2.6)}$$

where

$$F = F(z, \theta_B, \theta_B{}') = \frac{t\theta_B}{4} + \frac{{s_h}^3}{6}\left(\frac{d\theta_B}{dx}\right)^2 \quad \textbf{(2.7)}$$

The general solution of this equation is

$$\theta(x) = \frac{3}{8}\frac{t}{{s_h}^3}x^2 + Ax + B \tag{2.8}$$

With aid of the end conditions $\theta(0) = 0$ and $\theta(L) = \theta_B$, the two integration coefficients A and B can be determined with the following equation.

$$\theta(x) = \theta\frac{x}{L} + \frac{3}{8}\frac{t}{{s_h}^3}x(x - L) \tag{2.9}$$

In addition, because the slope of the flange is continuous at each end, the derivative of the change in the angle along the x-axis $\theta(x)$ is zero at both ends, $x = 0$ and $x = L$. The condition $\theta(0) = 0$ leads to the following expression for the length of the deformation zone

$$L = \sqrt{\frac{8 \cdot {s_h}^3 \cdot \theta}{3t}} \tag{2.10}$$

According to this expression, the deformation length between two consequent forming stations in roll forming depends on the web height s_h, bending angle θ and the sheet thickness t. The material specifications have no influence on the deformation length. Bhattacharyya suggests that the deformation length calculated by this equation agrees very well with the experimental values.

2.1.4 Elastic strain development in roll forming

In order to define the longitudinal strain in the deformation zone, the proportion between the deformation length L and the length of the edge of the strip $L*$ has to be calculated as follows.

$$\varepsilon = \frac{L* - L}{L} \tag{2.11}$$

There are different models to define the elastic strain in roll forming.

2.1.4.1 Linear model

Following figure shows the theoretical flow of the sheet metal while forming a U-channel in roll forming (Fig 2.13). While the bend line travels a straight line (L), the edge of the strip travels in a helical pattern (L^*). With a linear approach, the length of this helical pattern can be described as

$$L^* = \sqrt{L^2 + (s_h \cdot \theta)^2} \tag{2.12}$$

where s_h is the web height and θ is the bending angle. The elastic strain occurring between two consecutive stands in roll forming can be calculated using the equation (2.11).

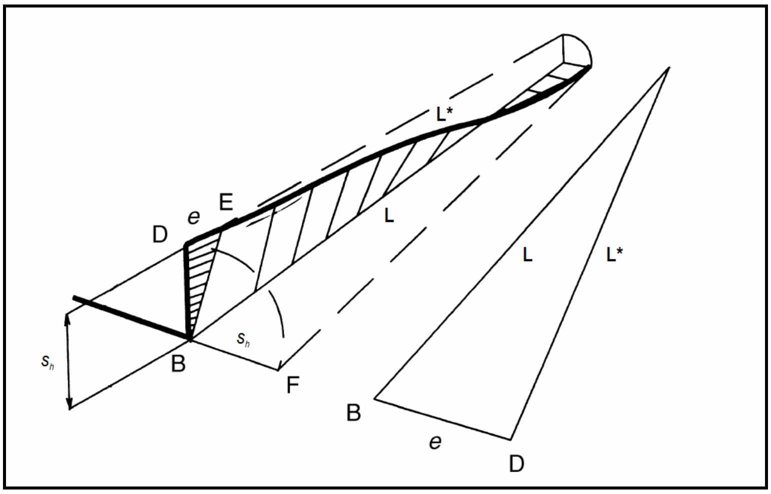

Figure 2.13: Schematic Representation of the Travel of the Sheet Metal during Roll Forming [4]

However, the path of the edge of the strip is not linear as described in the equation (2.12) (Fig 2.14). That's why actual values of elastic strain are higher than the values calculated with this method [4].

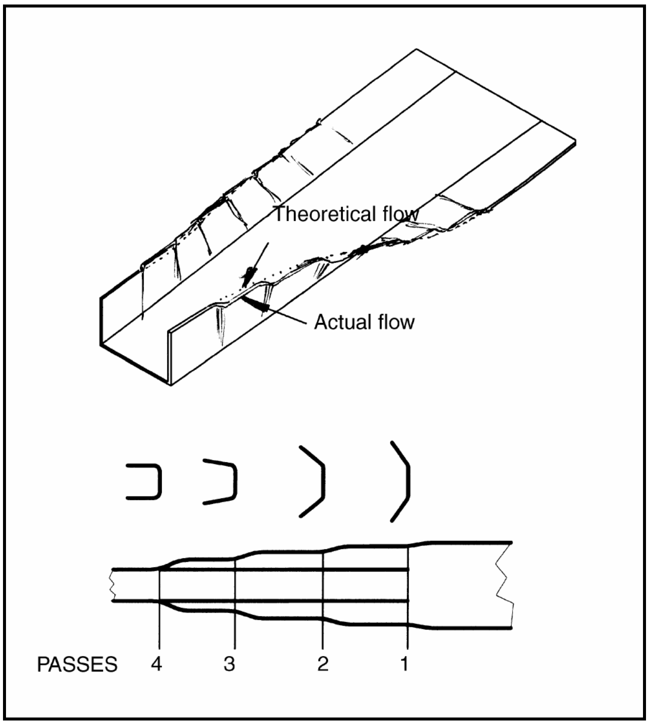

Figure 2.14: Schematic Representation of the Theoretical and Actual Flow of the Edge of the Strip [4]

2.1.4.2 Incremental model

During roll forming, every element of the sheet metal follows a spatial flow line between two consecutive forming stages. Following figure shows the coordinate systems used to describe the flow of these elements in roll forming analytically (Fig 2.15). In this figure, the coordinates X, Y, Z refers to the coordinates of the elements which are in the neutral curved surface or the deformed strip. Neutral curved surface is the curved surface which is located in the middle of the thickness of the strip. Hereafter, this will be denoted as DCS (deformed curve surface). Here, the x-axis coincides with the longitudinal axis of the system. X_1 refers to x-coordinate of the elements at the # (i) station and X_2 refers to the x-coordinate of the elements at the # (i+1) station.

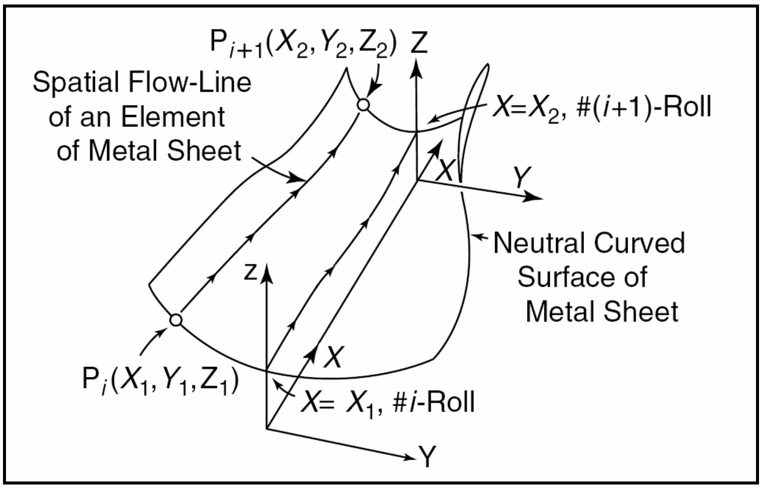

Figure 2.15: The Coordinate Systems of the Deformed Curve Surface [4]

In order to illustrate the 3-D flow of the strip between two consecutive forming stages, a normalized "shape function" $S(X)$ is defined as follows [9].

$$S(X) = \sin[(\pi/2)\cdot(X^*/L)^n] \tag{2.13}$$

where $X^* = X - X_1$ and $L = X_2 - X_1$.

The values of the "shape function" changes from 0 to 1 while the strip moves from one station $(X = X_1)$ to the next station $(X = X_2)$.

The values of the "shape function" is highly depended on the values of "n". The figure below shows different shape function patterns with varying values of the parameter "n".

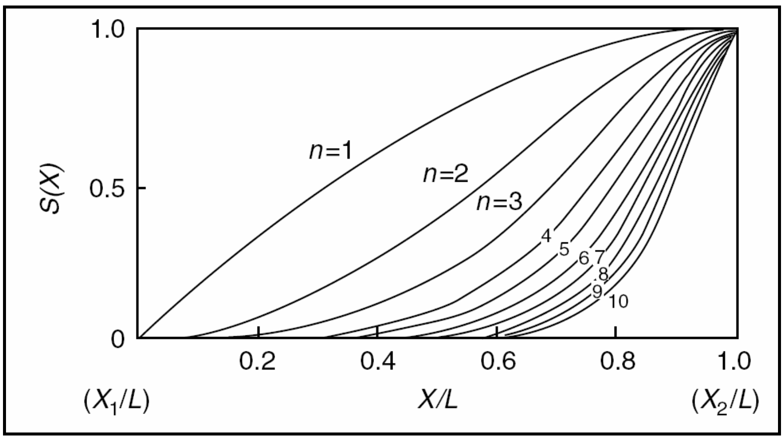

Figure 2.16: "Shape function" with Varying Values of the Parameter "n" [4]

With the aid of the "shape function", DCS of the strip between two consecutive forming stations is defined as follows [9].

$$X = X_1 \sim X_2$$
$$Y = Y_1 + [Y_2 - Y_1] \cdot S(X) \qquad \textbf{(2.14)}$$
$$Z = Z_1 + [Z_2 - Z_1] \cdot S(X)$$

These equations are derived with the following assumptions concerning the boundary conditions.

– The cross section of the profile of the semi formed strip at each roll gap center coincides with the roll profile, respectively.

– Every portion of the strip passes by the roll gap center along a horizontal flow line.

With the equations above, the path of every strip element in between two consecutive forming stages is defined. In order to calculate the strain occurring in the strip, the deformation in every portion of the strip has to be analyzed. Starting point of this analysis is the deformation of a strip with an original length of Δl_0 and a width equal to the original strip width. This strip is investigated incrementally while it is moving from the # (i) forming station to the # (i+1) forming station along DCS. Following assumptions are made in the calculations [9].

– Cross section of the entry side and the exit side of the deformed strip is embraced by the roll planes at every forming step.

– The forces on the strip between two stands which are acting in longitudinal direction are equal to the tension or compression acting on the strip between the same stands.

– The forces on the strip which are acting in transversal direction are in balance.

In order to analyze the deformation process in between two consecutive forming stations, the process is divided into appropriate numbers of deformation steps. In each step, the behavior of the strip elements which are divided in the transversal direction along the DCS will be investigated [9].

The investigated deformation step will be denoted as the (k)th step. The notations of the different nodes can be seen in the figure below.

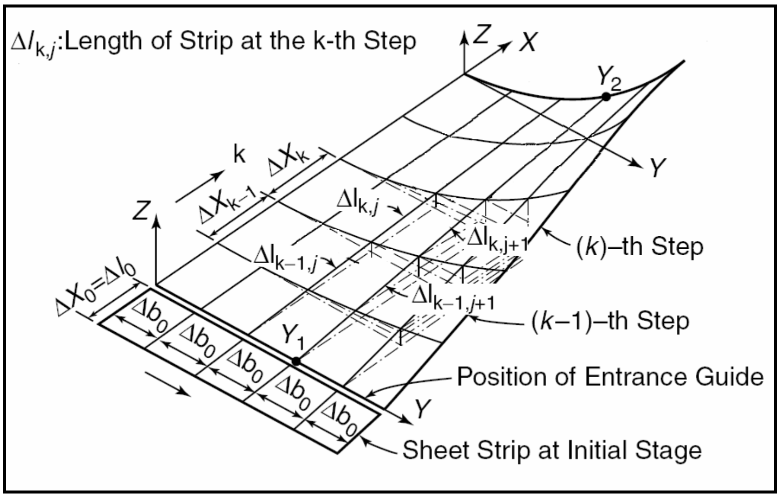

Figure 2.17: Notations of the Strip Elements [4]

The longitudinal membrane strain at the (j)th element at the (k)th step can be calculated with the following equations [9].

$$(d\varepsilon_{xm})_{k,j} = \left(\Delta l_{k,j} - \Delta l_{k-1,j}\right) / \Delta l_{k-1,j} \qquad \textbf{(2.15)}$$

where,

$$\Delta l_{k,j} = \left(\Delta X_{k,j}{}^2 + \Delta Y_{k,j}{}^2 + \Delta Z_{k,j}{}^2\right)^{1/2}$$
$$\Delta X_{k,j} = X_{k,j} - X_{k-1,j}$$
$$\Delta Y_{k,j} = Y_{k,j} - Y_{k-1,j}$$
$$\Delta Z_{k,j} = Z_{k,j} - Z_{k-1,j}$$

2.1.5 Roll design

In roll forming, the aim of a roll designer is to design the appropriate rolls and the process to realize the desired shape of the profile. This is a highly designer oriented phase. However nowadays, some software packages exist to assist the designer. COPRA RF of “data M” and PROFIL of “UBECO” are two examples of these. Calculation of the process related stress and strain situations creates the basics of the roll forming software.

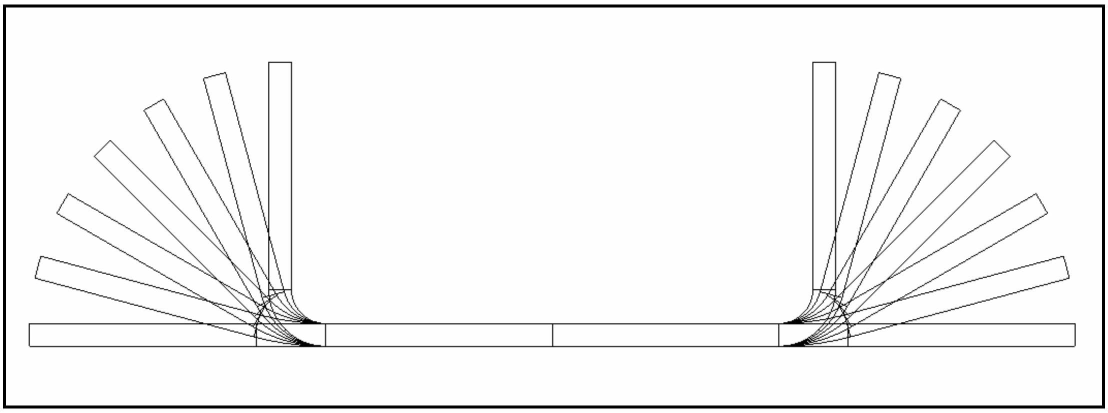

Figure 2.18: Flower Diagram

First part of the design process includes the design of the flower diagram. While doing that, parameters like sheet metal thickness, materials mechanical properties are taken into consideration. Following that, the actual roll design takes place.

Besides presenting the stress and strain conditions in the profile, these software packages have additional specifications including machining code generation for NC machines.

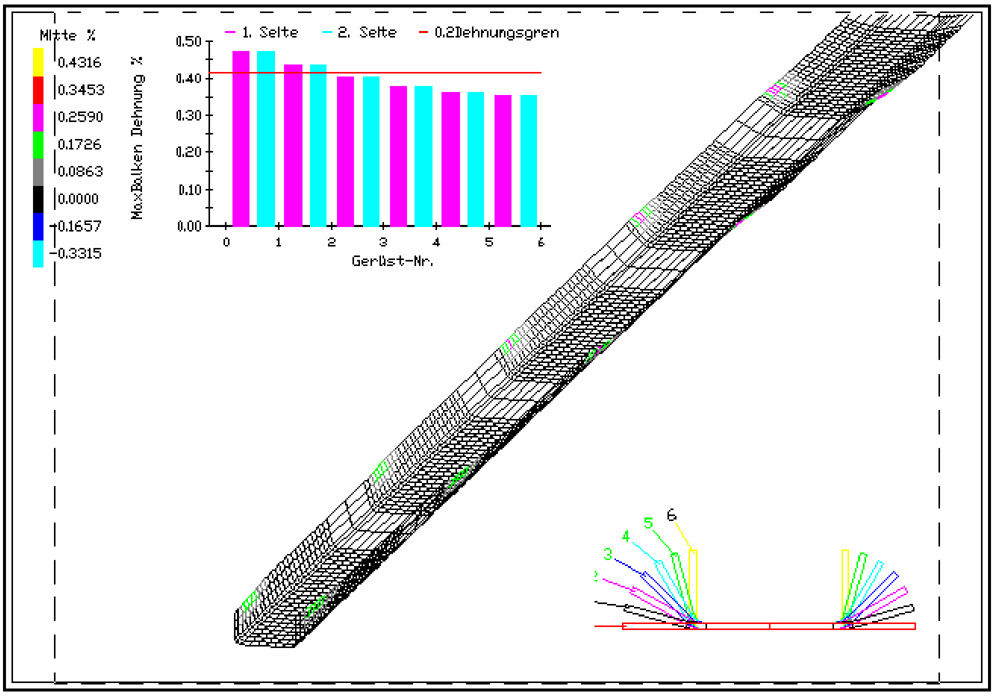

Figure 2.19: Strain Analysis with COPRA RF

Both software packages have FE program interfaces which enable the generation of the FE model of the entire process. The generated model can be solved using different FE softwares.

2.2 Linear Flow Splitting

Linear flow splitting is a new mass forming process for the production of bifurcated profiles in integral style. The semi-finished product is a plane sheet metal which is transformed at ambient temperature by a specific tooling system, consisting of obtuse angled splitting rolls and supporting rolls (Fig. 2.19). The fixed tool system forms the work piece while the piece itself is being moved through a series of steps. The result is a profile with final geometry.

The bifurcations emerge from a surface enlargement of the sheet metal's band edge during material forming. The bifurcated profile is marked by a web and two flanges. The surface beneath the splitting roll is defined as the upper side [10].

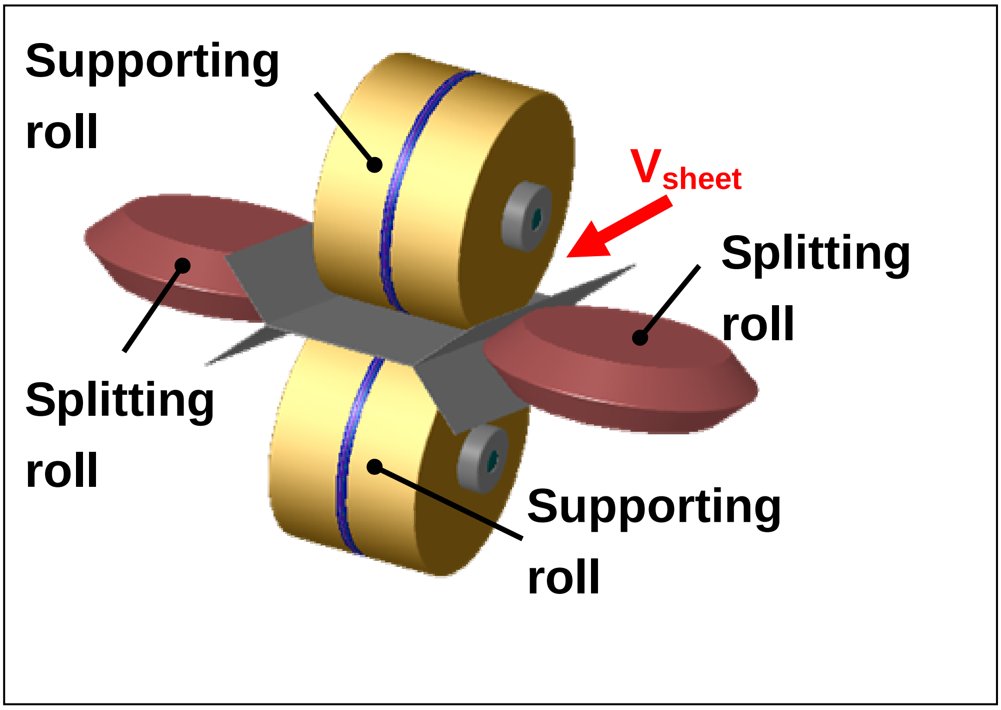

Figure 2.20: Schematic Representation of the Linear Flow Splitting [10]

With this method, a rigid structure is obtained at the flange section of the split profile. Studies show that the hardness is increased in the flange as a result of the splitting process. Hardness values reach a maximum value along 1-3 line (Fig. 2.20) in the middle section of the flange while they decreases at the end sections of the flange. The hardness values also decreases along 2-4 line (Fig. 2.21) in sheet metal direction [11].

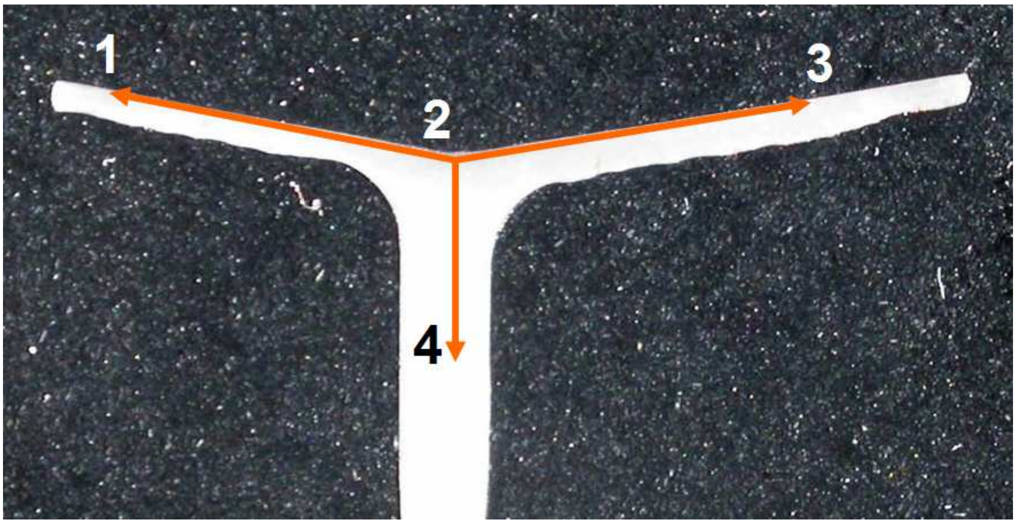

Figure 2.21: Section View of the Splitted Profile [11]

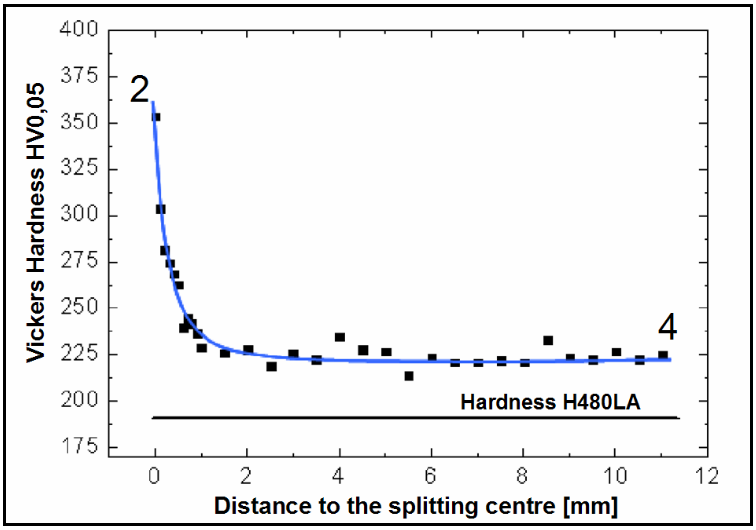

Figure 2.22: Hardness in the Splitted Profile along the 2-4 Line [11]

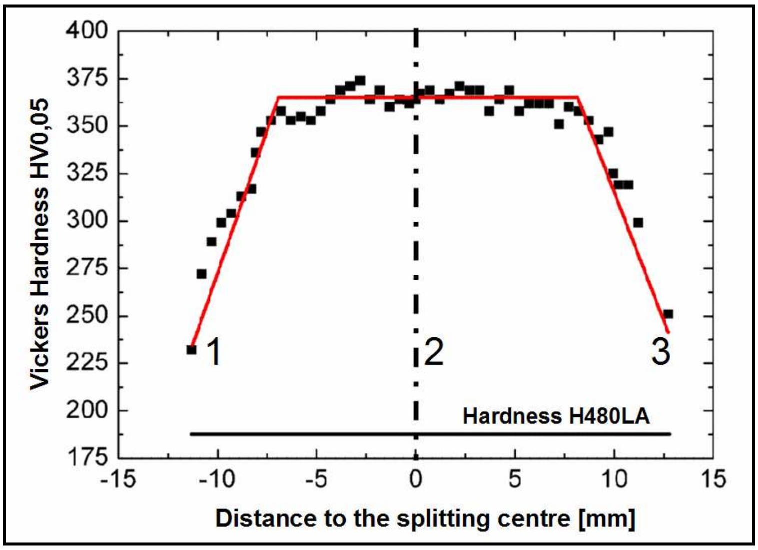

Figure 2.23: Hardness in the Splitted Profile along 1-3 Line [11]

2.3 FE Simulation of the Forming Process

With the usage of the finite element method (FEM) in forming, it is aimed to model a forming process in order to investigate the stress and strain conditions occurring in the deformed part, tool or the complete system. With the aid of the FEM, for instance, the variations of different parameters in one process can be obtained without long and costly experiments.

FEM is a numerical computation of partial differential equations which represent the physical specifications of an existing physical problem. It is based on the division of the problem area in to finite number of elements. The solution of the differential equations incrementally according to the start and boundary conditions gives the desired stress and strain situations.

FE analyses are divided into two categories; linear and nonlinear. In the linear analyses, equations matrix is constant. For instance, in a linear analysis, the displacement is proportional to the force applied. However, in the nonlinear analyses, the behavior of the investigated part is dependent on the material properties. Main reasons of the nonlinearity are material properties, geometrical properties and the contract conditions in the systems [12].

2.4 GOM/Argus Optical Measurement System

For the measurement of the strain values in deformed sheet metal parts, measuring system GOM/ARGUS exist at PtU. In order to measure the strain values in a deformed sheet metal part with this system, first circular dots with regular spacing of 1 mm to 5 mm are applied to the original sheet metal with electrochemical etching, laser etching or printing method (Fig 2.23). Applied dots remain even after a large deformation of the metal part and so they represent the flow of the material. Afterwards, the centres of these dots are used to determine the deformation occurred in the part. Recording of the deformed part with a digital CCD camera from various views follows the forming process. These images are used by photogrammetric algorithms to determine the coordinates of the dots on the sheet metal part. The determined coordinates of the dots are used to create a mesh by assigning the centre of the dots to the neighbors (Fig. 2.24 and 2.25). After that, the strain tensor is determined by comparing, for instance, each 2x2 point field in this mesh with original geometry (Fig. 2.26). Consequently, the major and minor strain and the thickness reduction of the sheet metal can be obtained as surface information. The thickness reduction is directly calculated using the major and minor strain with the assumption of a constant volume [13].

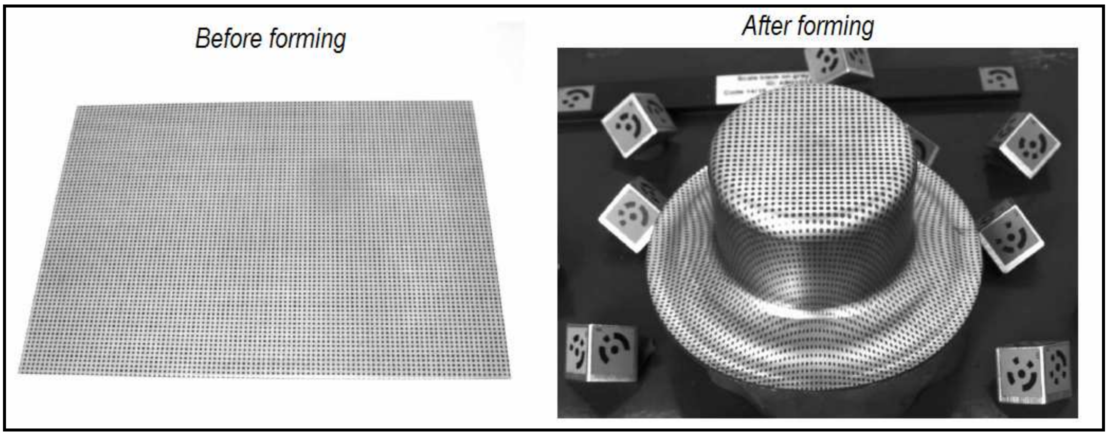

Figure 2.24: Example of the Sheet Metal with Dots before and after the Forming [13]

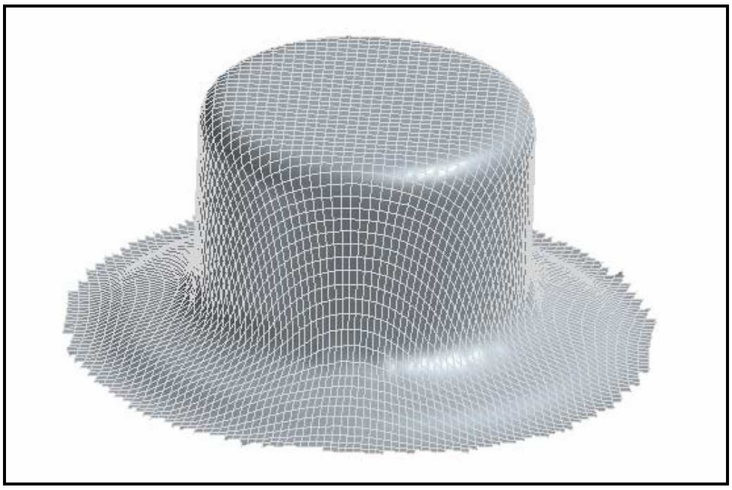

Figure 2.25: Created Mesh after Point Calculation [13]

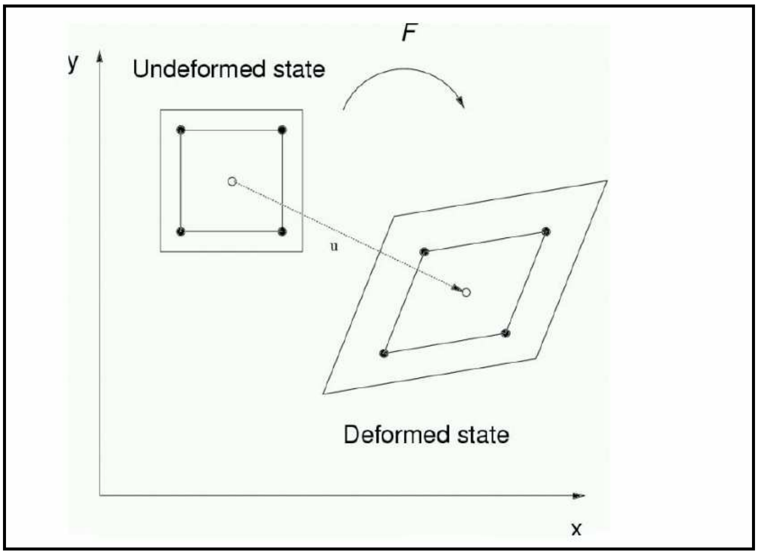

Figure 2.26: Calculation of the Surface Strain Tensor [13]

3. PROBLEM STATEMENT, MOTIVATION, OBJECTIVES AND STRATEGY

Constant cross section beams (profiles) with bifurcated cross sections are widely implemented and used in the current technology. As popular examples T- and I-profiles are employed both in the field of civil engineering and as structural elements in automobile, boat and instrument panel construction.

The new massive forming method, linear flow splitting enables the production of bifurcated structures from sheet metal without joining seams, material duplications or heating of the semi-finished product. The reprocessing of splitted profile in the following rolling, or roll forming, process enables continuous production of absolutely new profiles (Fig 3.1). For the analytical design of roll geometries for roll forming, exists a number of CAE program systems. Essence of these systems is analytical design of the forming geometry and evaluation and optimization of the resulting roll geometries. For this purpose string models with polynomial approaches are used. However, up till now, integral bifurcated profiles are not apprehended analytically**.**

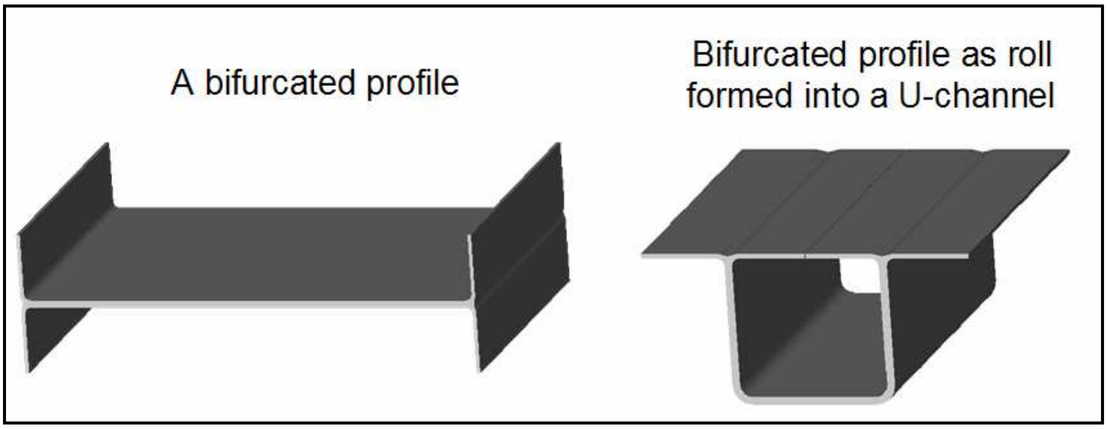

Figure 3.1: Bifurcated Profile as Semi-Finished Product and as roll formed into U-Channel

Goal of this project is to develop an analytical model for the roll forming of bifurcated profiles. At the beginning, within literature survey, appropriate computation parameters are determined. On the basis of these values numerical models are developed and analytical relations are derived. In the second step, in an industrial case study, for the estimation of the required sequential steps analytical approaches and guidelines have to be determined. Validation of the formals can be conducted in the test of the model. Finally, design guidelines concerning forming strategies and tool design by the reprocessing of the roll forming for multi-chamber profile shall be derived. For this purpose, an appropriate roll set will be designed, made and tested.

In this study, it is aimed to derive analytical relations in roll forming of bifurcated profiles by adapting an FE approach. Therefore, it is necessary to validate the FE simulations. This will be achived by comparing the principle plastic strain values in bending zone from the simulation and the experiment. For the experiment, the roll forming machine and the roll forming tool in SFB 666 Hall at PtU will be used and thus, additional costs will be spared. For the FE simulation, the same process will be modeled.

The variation of the geometric and forming related parameters, such as web height, flange length and bending sequence with FEM follows the determination of the appropriate FE modeling concept for the roll forming of bifurcated profiles. Using the variations of the collected data, an emprical formula for the longitudinal strain which occurs during roll forming of bifurcated profiles will be derived.

4. BASIC APPROACH ANALYSIS FOR THE FE MODEL

FEM is a strong tool to analyze the strain and stress distribution occurring in the sheet metal during roll forming. In this method, the sheet metal is divided into many elements which are to be analyzed discretely. The accuracy of the simulation highly depends on the size of the elements. Convergence rate to the real values usually increases while the element size decreases. On the other hand, number of elements affects the duration of the simulation adversely. If the element number is doubled, simulation time quadruples. Therefore, it is necessary to optimize the simulation time by decreasing the element number without worsening the results.

In order to determine the optimum element size or that is to say number of elements, the appropriate modeling concept has to be defined. Hence, in following chapters, two different concepts will be compared.

4.1 Basic FE Model for the Forming of the Bifurcated Profile

In order to derive analytical relations in roll forming of bifurcated profiles, a basic FE model has to be selected and the selected model has to be validated with the experiments. Therefore, the roll forming tool and the corresponding profile geometry in the SFB666 Hall at PtU will be used to select an appropriate basic FE model. Thus, the additional tooling costs for the experiments will be saved.

Many FE modeling concepts have been presented so far for analyzing of roll forming process. Tehrani et al. used shell elements to model the sheet metal and the simulations made use of explicit version of ABAQUS 6.4 [14]. Lindgren used finite element package MAR/MENTAT to simulate the roll forming process and used four-node shell elements to model the metal strip [15].

The FE model of the process is generated with the software package MARC/MENTAT 2005r2. With the user interface of this program, it is possible to model deformable bodies, sheet metal in this case, as well as rigid ones. Moreover, the FE related parameters, such as material properties, solver type, increment size, etc. can be defined by using this interface.The tool geometries are modeled as rigid surfaces. In order to simplify the FE model, only the 60^0 portion of the cylindrical tools is modeled which actually comes into contact with the sheet metal (Fig 4.1). The radii of the rolls are designed as the real ones, namely 150 mm for the upper rolls and 120 mm for the lower rolls. There are 20 separate rolls in total including the two entry rolls and the two intermediate idler rolls between the last two forming stages. The distance between two consecutive stands in the model is as in the roll forming line 400 mm. In the model, in contrary to the real process, the rolls are driven upon the sheet metal (Fig 4.2).

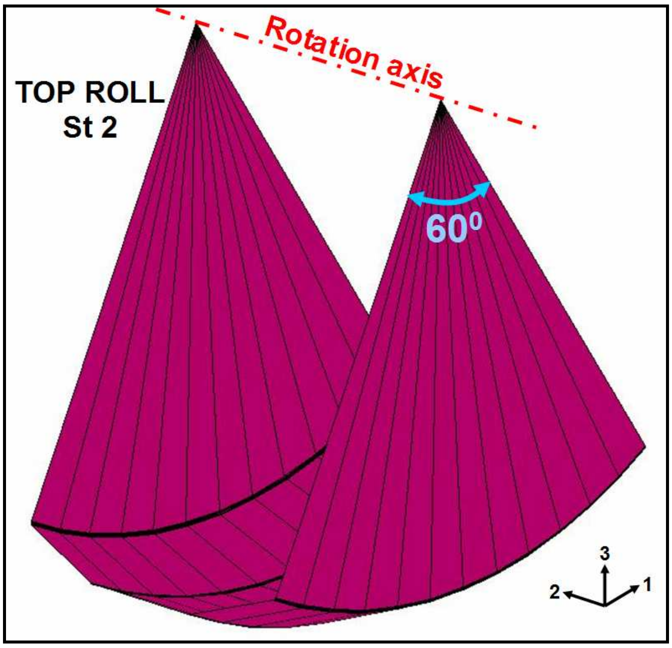

Figure 4.1: FE Model of a Roll Forming Tool

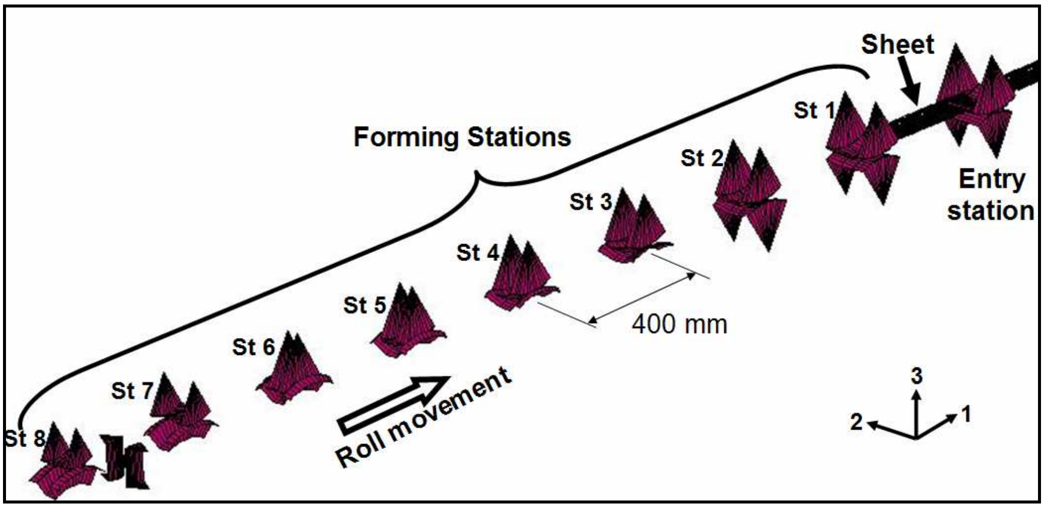

Figure 4.2: FE Model of the Roll Forming Tools

As in the real process, 8 forming stages are used in the FE model. At the end of the roll forming process, the bifurcated profile is bent 85^0 in both sides. The bending sequence is shown in Table 4.1.

Table 4.1: Bending Sequence of the Bifurcated Profile

	0→1	1→2	2→3	3→4	4→5	5→6	6→7	7→8
Bending Angle	8	11	11	11	11	11	11	11
Total Bent Angle	8	19	30	41	52	63	74	85

Since the sheet metal is a deformable body, it is modeled with elastic-rigid strain hardening plastic elements. First, the existing geometry of the cross section of the bifurcated profile is composed via a Python script and meshed with surface elements. Because the semi finished product, namely the bifurcated profile and the end product after roll forming are symmetrical, only one half of it will be modeled (Fig. 4.3).

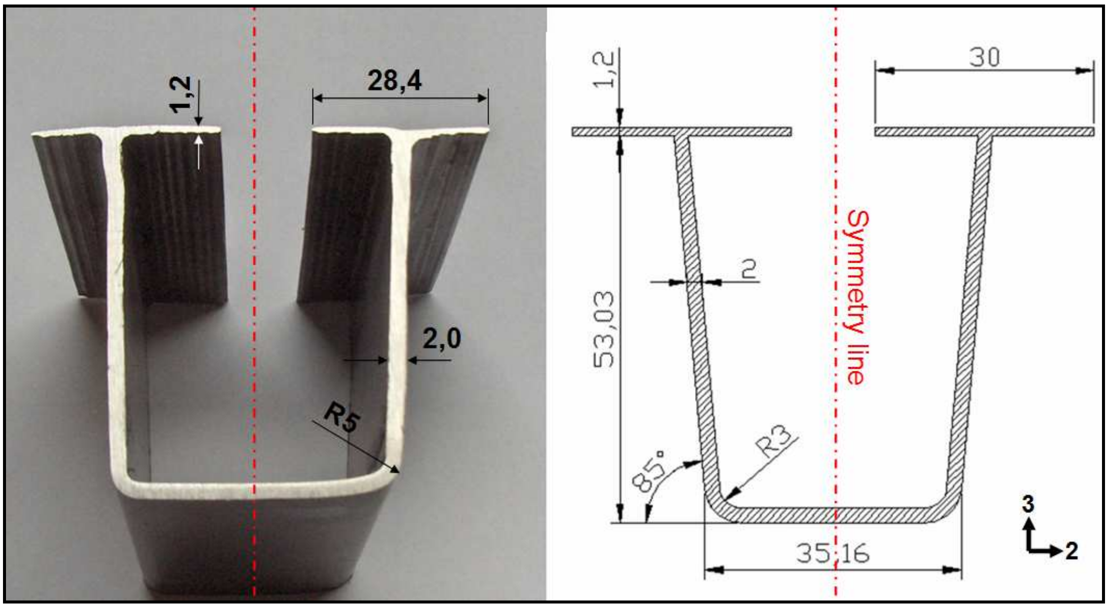

Figure 4.3: Cross-Section of the Roll Formed Bifurcated Profile

Two different meshing concepts which differ from each other in the element numbers in the bending line will be investigated. Therefore, two sheet models are generated via a Python script (Fig. 4.4). The advantage of the model generation via a Python script is the convenience of the variation of the geometrical parameters.

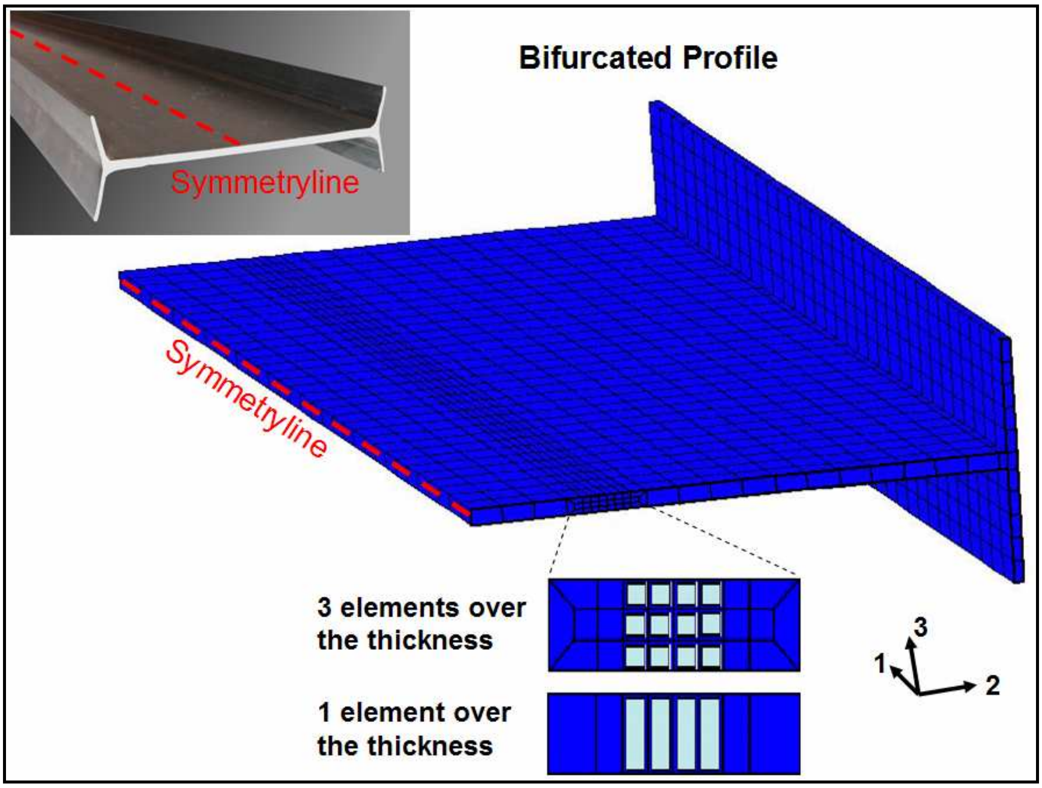

Figure 4.4: Cross-Section of the FE Model of the Bifurcated Profile

After modeling of the bifurcated profile as a meshed surface, three dimensional elements are generated by expanding the two dimensional ones. Thus, elements with a depth of 5 mm are generated. These elements have a width of 4 mm and a height of 2 mm outside the bending line. The flange section of the profile is modeled with elements having a width of 1.2 mm which corresponds to the thickness of the flange and a height of 2.8 mm. In the bending region, the elements have a width of 1 mm and a height of 2 mm in a variation and a height of 0.66 mm in another variation. As mentioned before, all elements have a depth of 5 mm.

Element properties are defined with “Type 7”, which is an eight node, isoparametric, arbitrary hexahedral, three dimensional brick shaped element type. Although, it has pour shear (bending) characteristics it may be improved by using alternative interpolation functions such as “Assumed Strain”. Assumed Strain formulation enables the element take a so called hourglass shape. That’s why this formulation is used for all elements. Additionally, in order to eliminate the potential element locking “Constant Dilatation” method is implemented [16].

The FE model of the sheet metal has a length of 1300 mm which is 100 mm higher than the distance between four forming stations. Thus, it is possible to investigate the strain and stress conditions in the middle of the sheet during the entire simulation while the sheet is still in contact at least with three forming stations.

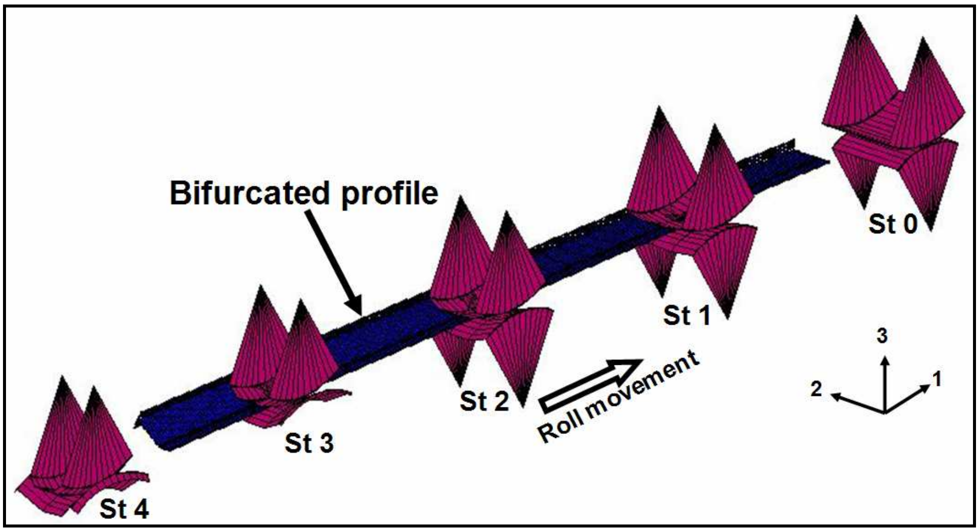

Figure 4.5: Sheet Model in-between Roll Forming Tools

Three boundary conditions which fix the node displacement in different directions are defined for the FE model of the sheet metal. The BC in the first direction, namely in longitudinal direction, ensures the fixation of the sheet metal model while the rolls are driven upon it. This is defined only on the nodes of the sheet which are on the entry side of the rolls. The BC in the second direction, namely in the transversal direction, is used to define the symmetry of the part. The BC in the third direction fixes the sheet in the thickness direction. This is defined only on the entry and the exit side of the sheet on symmetry plane (Fig 4.6).

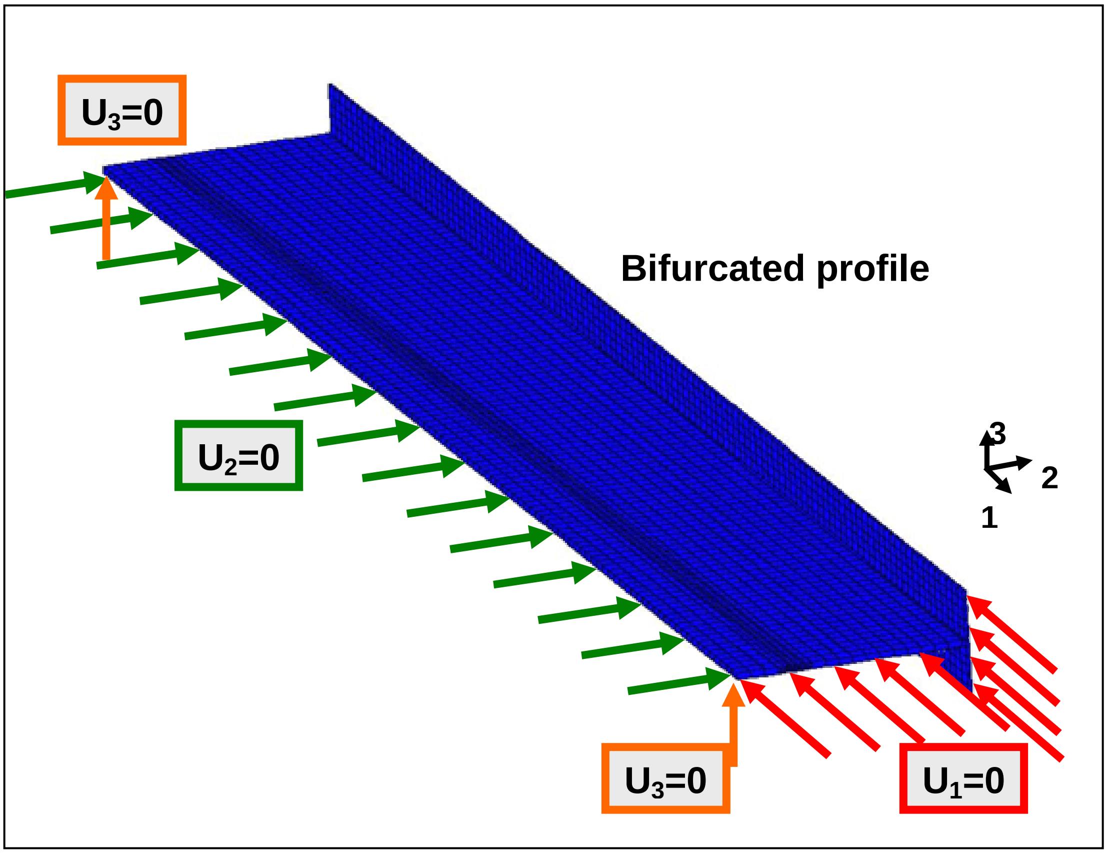

Figure 4.6: Boundary Conditions on the FE Model of the Bifurcated Profile

The longitudinal elastic strain caused by the plastic deformation of the part is the main concern in the simulation; therefore the behavior of the material in plastic region has to be defined. The flow curve is the main tool to describe the plasticity of the material. The flow curve is determined via tensile test. However, stress values taken from the tensile test are limited to a certain strain value. In order to extend these stress values, Swift's equation is used.

$$\sigma = K \cdot (\varepsilon_0 + \varepsilon)^n \qquad \textbf{(4.1)}$$

In this equation, K is the strength index and n is the strain hardening index. These are material related parameters which have to be fit to the existing tensile test values. The ε_0 value is calculated as follows

$$\varepsilon_0 = \left(\sigma_y / K\right)^{\left(\frac{1}{n}\right)} \qquad \textbf{(4.2)}$$

However, it is known that by fitting the Swift's equation to the real material values a small fitting error is made. Therefore, while defining material properties for the elements, first the tensile test results are taken; afterwards the flow curve is extended via Swift's equation (Fig. 4.7) for the steel H480LA. Young's modulus of this material is 210000 MPa and Poisson's ratio is 0.29.

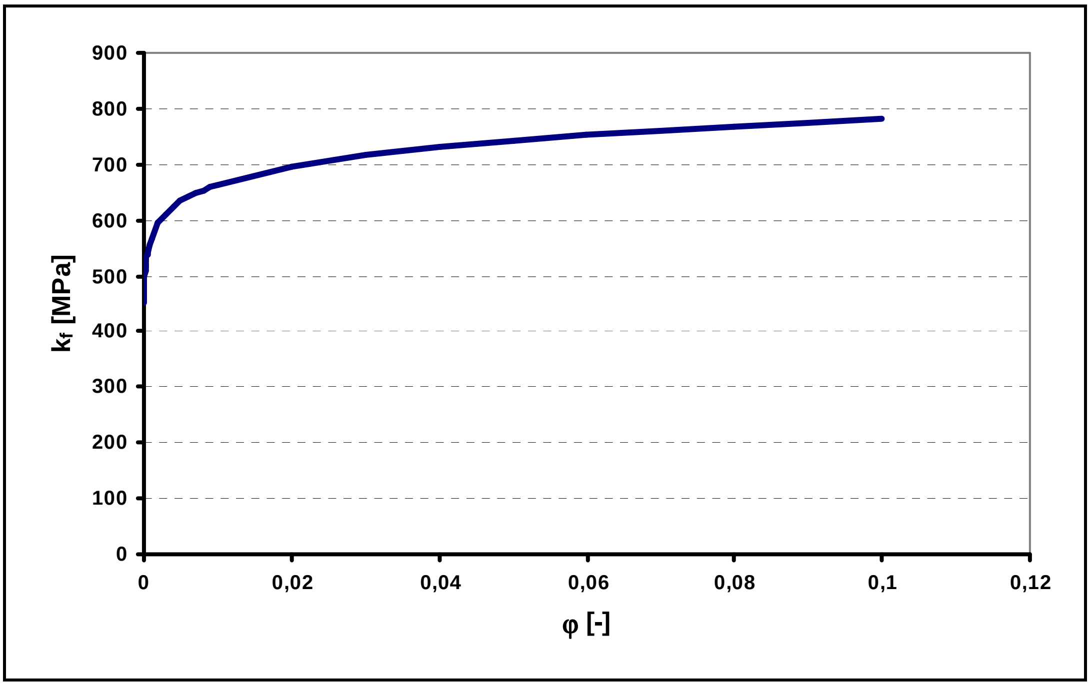

Figure 4.7: Flow Curve of the Material H480LA

In the FE model, also the contact conditions have to be defined. There are three options for this definition; no contact, sliding contact and gluing. Since the only deformable body, the sheet metal comes into contact with all of the rolls the contact conditions are defined between sheet and the rolls as "Touching". By the definition of the contact, it has to be ensured that only the outside surface of the rolls touch the sheet.

Contrary to the real process, in the simulation, the contact between the sheet and the rolls is assumed to be frictionless. Therefore, it is not necessary to define the friction coefficient μ between contact bodies.In the simulation, sheet metal model stands still and the rolls are driven upon it. Therefore, a constant displacement in the first direction, namely the longitudinal direction is defined for all of the rolls which corresponds to the forming velocity 3.5 m/s.

4.2 Validation of the FE Simulations

The FE simulations will be validated by comparing the principal logarithmic plastic strain values along a line in transversal direction at the outside surface of the profile of the experiment parts and the simulation results.

To measure the plastic strain in the experiment part GOM/Argus measurement system was used. First, circular dots with a regular spacing of 1 mm and a radius of 0.5 mm are applied to the surface of the bifurcated profile by electrochemical etching. These dots will be used to demonstrate the material flow after forming. Record of the deformed dots follows the forming. The displacement of these dots respective to the neighboring ones gives the plastic strain values in major and minor direction (Fig 4.8).

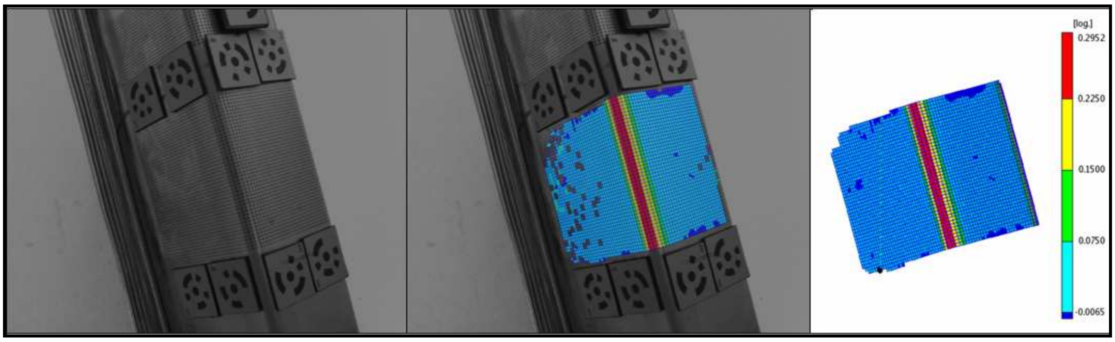

Figure 4.8: Plastic Strain Measurement via GOM/Argus Measuring System

For the experiment, approximately 1500 mm long precut bifurcated strips are prepared. The length of the strip corresponds to the length of the bifurcated strip in the FE model. Since the experimental part is not fixed in the symmetry line, deviations by the end profile geometry occur. Therefore, parts with 5 mm outer radius on the bend line are analyzed (Fig. 4.9). The 5 mm outer radius corresponds to 3 mm inner radius.

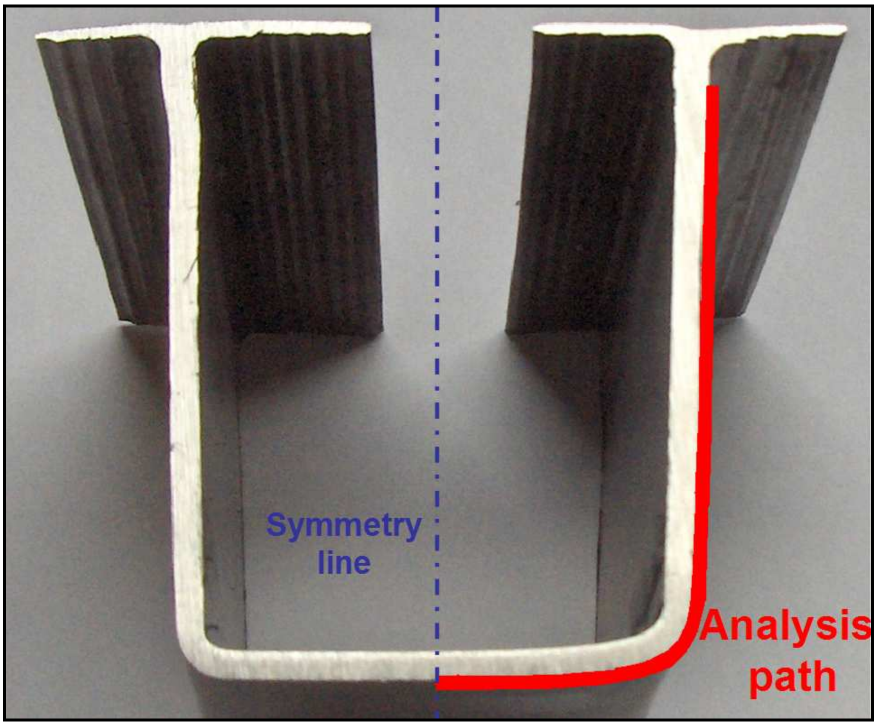

Figure 4.9: Analyze Path on the Experiment Part

On the FE simulation side, the major plastic strain values along the analysis path located in the middle of the sheet metal model will be analyzed. Since from the simulation, only the engineering plastic strain values can be read these values have to be converted into logarithmic ones with the following equation:

$$\varphi = \ln(\varepsilon + 1) \quad \textbf{(4.3)}$$

Because there are two different FE modeling concepts which differ from each other in the mesh in the bending zone, plastic strain values of these two concepts will be compared with the experimental results. (Fig 4.10) shows the results of two experiments with an outer radius of 5 mm and the results of the FE simulations with different meshing concepts.

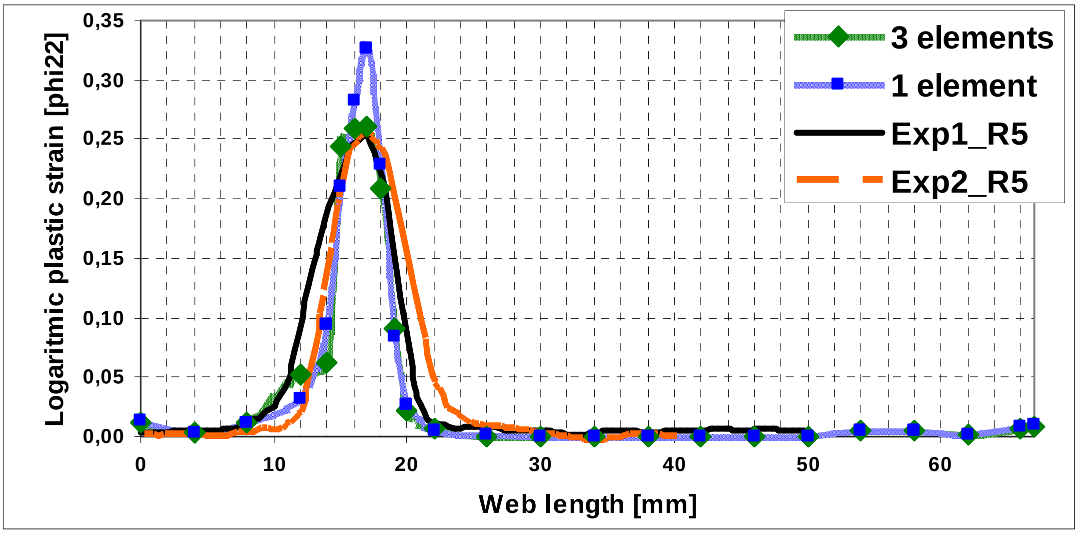

Figure 4.10: Major Logarithmic Plastic Strain along Analyze Path

The FE model with 3 elements over the thickness at the bending zone differs from the experiment values by about 1.5%. However, a deviation of 27% is noticed by the model with 1 element over the thickness. Consequently, the modeling concept with 3 elements over the thickness in the bending zone will be used in the further investigations. In this model, “Assumed Strain” formulation is used by the elements.

5. COMPARISON OF THE FLAT SHEET METAL AND BIFURCATED PROFILE

For a better understanding of the behavior of a strip with bifurcations on the edge during roll forming, strain characteristics of it will be compared with the ones of a flat strip. The comparison makes use of an FE tool. Therefore, the results of a FE simulation of a flat strip with the same geometry as the bifurcated profile except the flange at the end are needed.

5.1 FE Modeling

For comparison purposes, it is necessary to use the same modeling concepts. Therefore, the only difference between the flat sheet model and the bifurcated sheet model is the flange at the edge (Fig, 5.1).

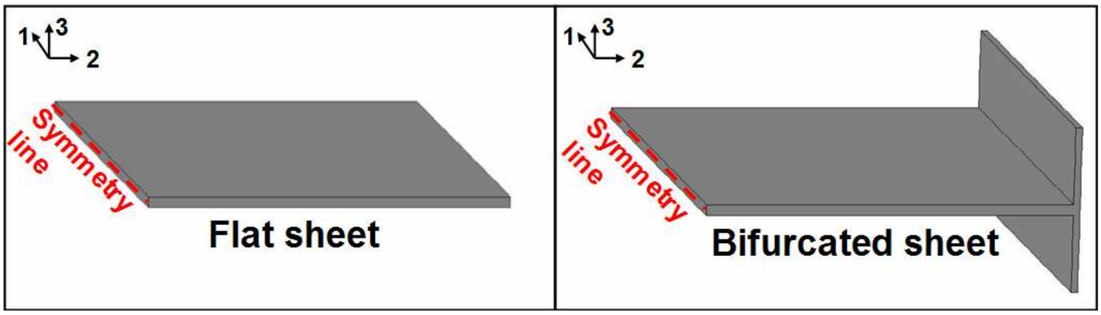

Figure 5.1: Schematic Representation of the Flat Sheet and Bifurcated Sheet

In order to provide equality of the two models, all the modeling work is performed using Python scripts. Generated FE models are solved with the solver of MARC/MENTAT 2005r2 (Fig. 5.2).

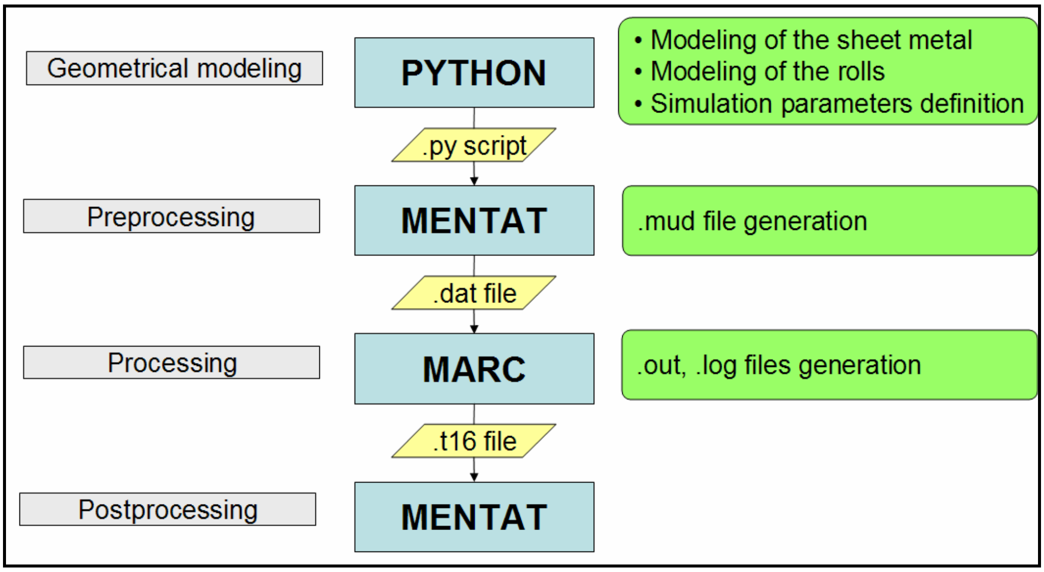

Figure 5.2: Workflow by Modeling of the Roll Forming Process

During the analysis of the simulations, not all forming stages will be used. In the real process, the bifurcated sheet is bent with top rolls in the last two forming stages. These two rolls do not support the profile on the bending line, but by pressing on to the flange section of it (Fig. 5.3). Therefore, additional strain and stress are induced in the flange section. This affects mainly the strain values at the edge of the flange which will be analyzed in this study. In order to prevent the effects of the top roll pressure on the flange, the last three forming stations will not be analyzed.

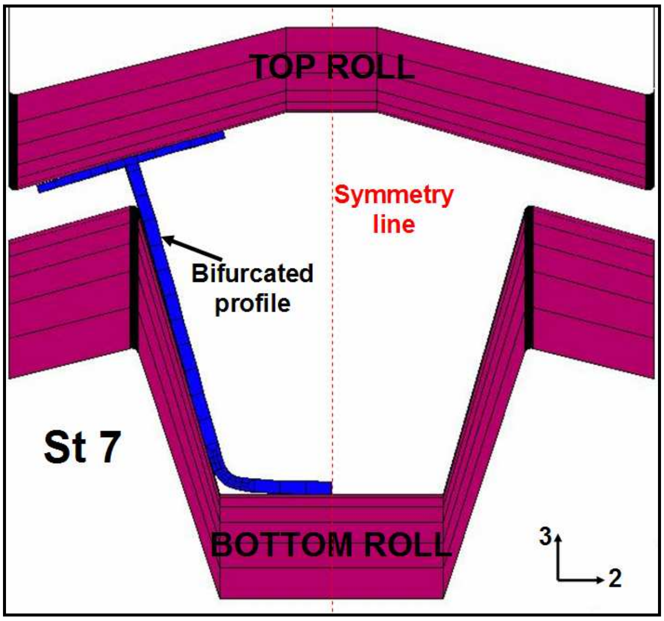

Figure 5.3: Cross-Section View of the 7th Forming Station (74^{0})

The bifurcated sheet is bent in 8 consecutive stages. The first stage has a bent angle of 8 degrees and all the others have a bent angle of 11 degrees. In order to eliminate the effects of the change in the bent angle; analysis of the strain values will start after the first forming station (Table 5.1). In following table, analyzed forming stages are indicated with a dotted pattern.

Table 5.1: Bending Sequence of the Bifurcated Profile

	0→1	1→2	2→3	3→4	4→5	5→6	6→7	7→8
Bending Angle	8	11	11	11	11	11	11	11
Total Bent Angle	8	19	30	41	52	63	74	85

5.2 Comparison of the Flat Sheet with the Bifurcated Sheet

In this section, mainly the longitudinal strain values at the flat sheet at the outer and inner band edge of the web will be compared with the ones at the bifurcated sheet at the outer and inner band edge of the web and the flange.

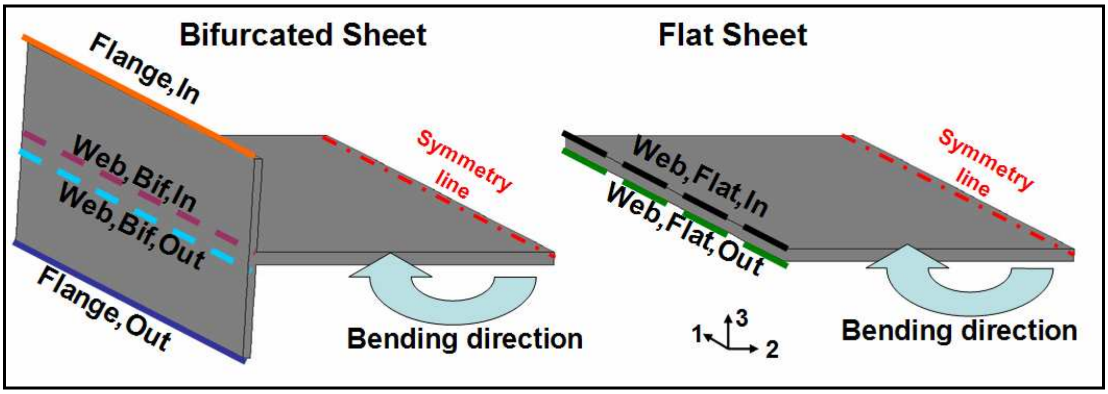

Figure 5.4: Analyze Paths on the Bifurcated and Flat Sheet

Strain values will be demonstrated in diagrams where the x-axis is the distance to the entry of the forming line. Here, the 1st forming station is taken as the starting point of the process, not the entry station. In the following figure, the numbers by the station numbers indicate the distances to the starting point.

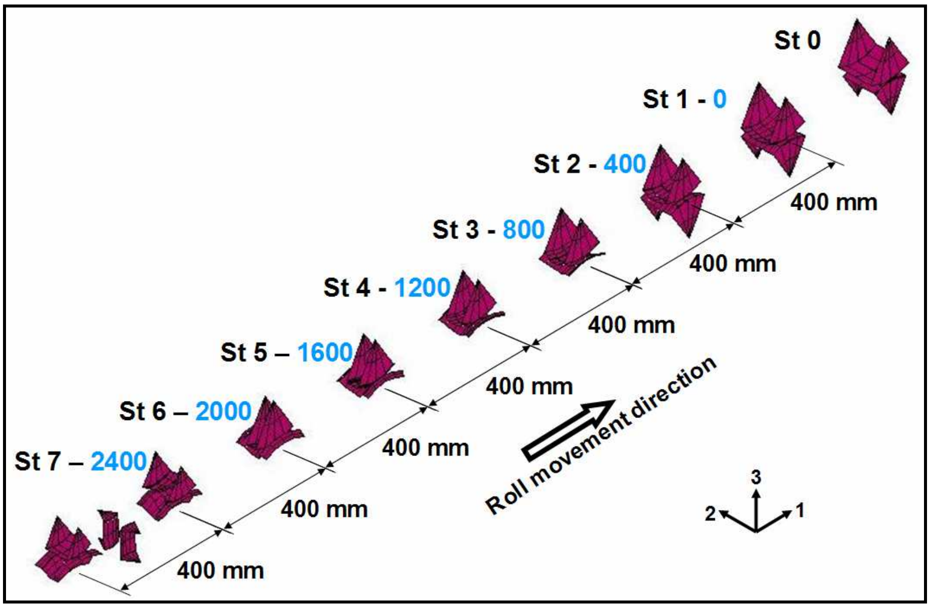

Figure 5.5: Schematic Representation of the Forming Station Distances to the 1st Forming Station

Figure 5.6 shows the longitudinal strain development during roll forming of the flat sheet strip. Here, it is observed that between to consecutive forming stations, the strain values of the outer band edge are under a certain level till a certain point. Then, it starts to increase to reach its peak and before reaching the forming station, strain values decrease back to zero or a very low level. This means that the sheet metal starts to bend after a certain point between two forming stations and before reaching the next forming station, it will be bent back. The longitudinal strain development for the inner side of the flat sheet strip is nearly the same as the outer side but with a sign change. This flow shows the same trend with the outcome of the previous studies [15].

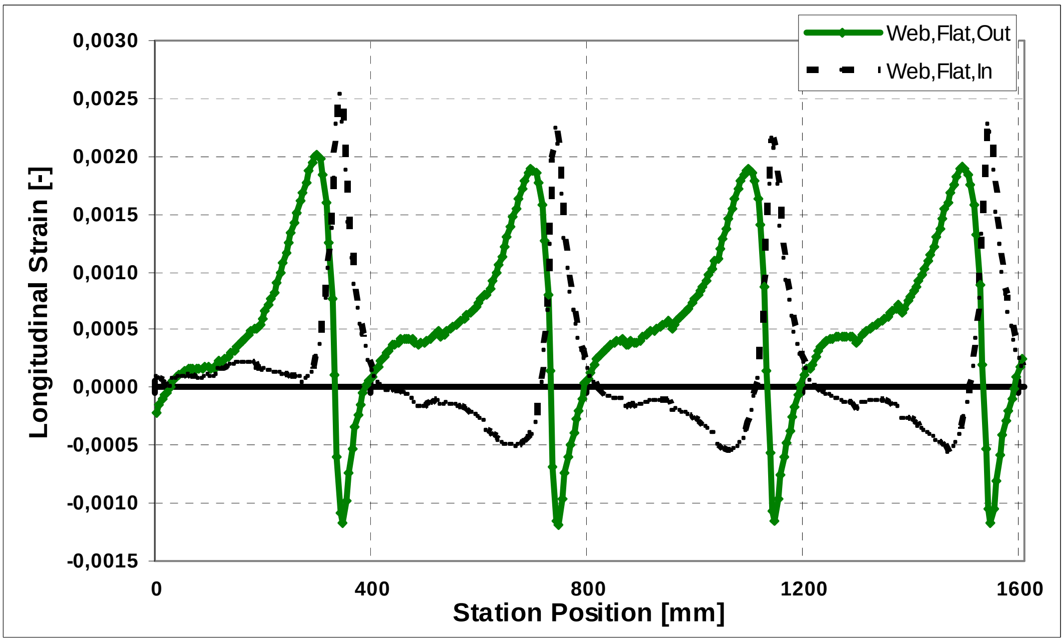

Figure 5.6: Longitudinal Strain Development in Flat Sheet

The path of the strip during roll forming can be defined with a so called “Shape Function” (See Chapter 2.1.4.2). Figure.5.7 shows the “Shape Functions” of the flat strip obtained from the FE simulation and the calculations. For the calculated “Shape Function”, the” *n* “value is taken as 4.3. The two lines match well with each other. In other words, the spatial flow of the flat strip between two forming stages during roll forming can be represented by a so called “Shape Function”.

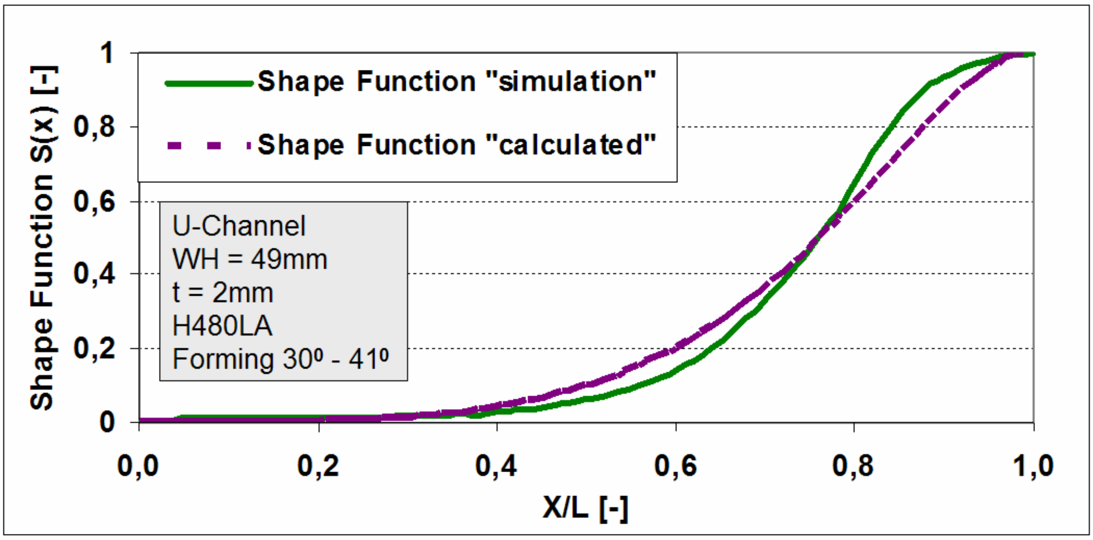

Figure 5.7: “Shape Function” of the Flat Sheet Strip Edge during Roll Forming of the U-Channel

If the longitudinal strain values of the flat strip and bifurcated strip at the edge of the web are compared (Fig. 5.8), it is seen that the strain values at the bifurcated strip are significantly less than the ones at the flat strip.

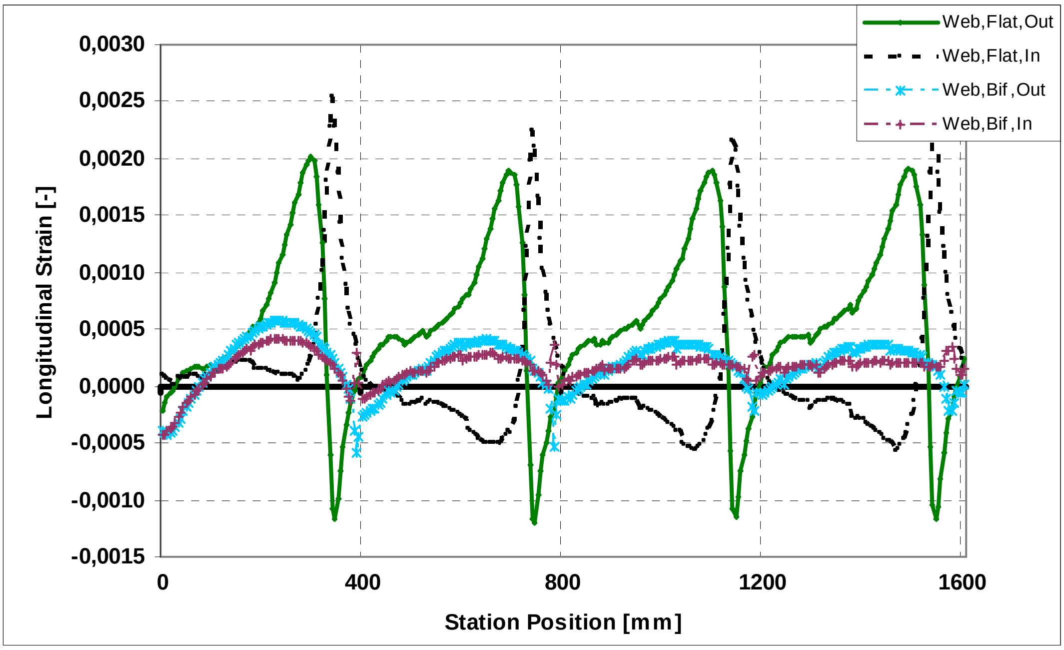

Figure 5.8: Comparison of the Longitudinal Strain Values at Web Edge (WH=49mm, FL=15mm)

As the longitudinal strain values at the band edge on the flange of the bifurcated strip are compared with the ones at the band edge of the flat strip (Fig. 5.9), two main points are noticed. Firstly, the maximum longitudinal values occurring in bifurcated strip at the band edge of the flange are less than the ones occurring in the flat strip at the band edge. This is indicated with $\Delta\varepsilon_{\max}$ in the Figure 5.10. Secondly, the maximum value of the longitudinal strain is closer to the forming station. The distance between maximum values of the strain in bifurcated sheet and flat sheet occurring during roll forming is indicated with ΔX .

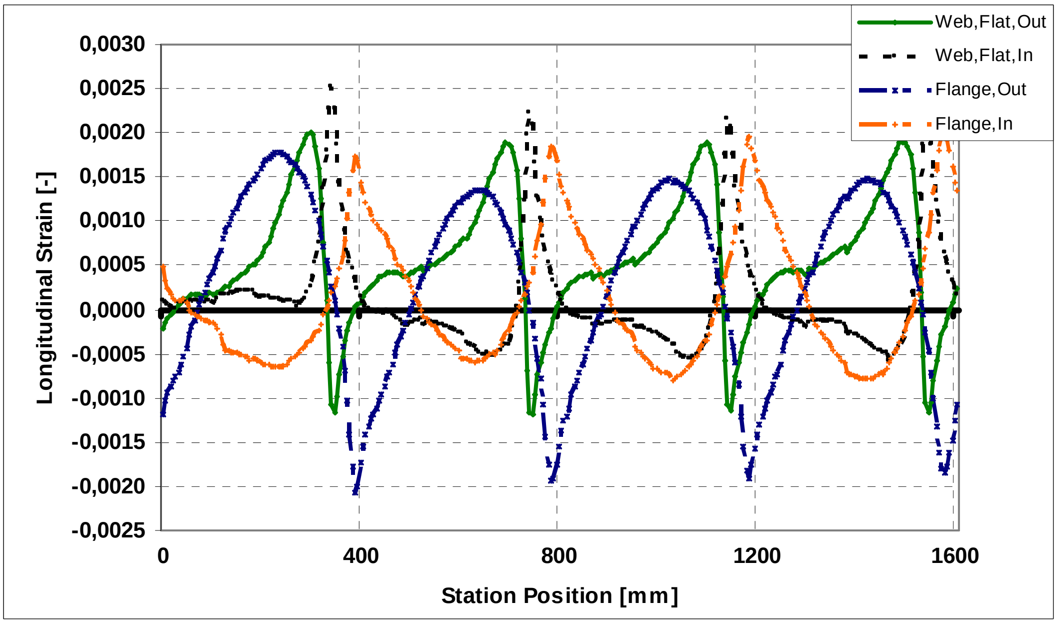

Figure 5.9: Comparison of the Longitudinal Strain Values at the Flange Edge (WH=49mm, FL=15mm)

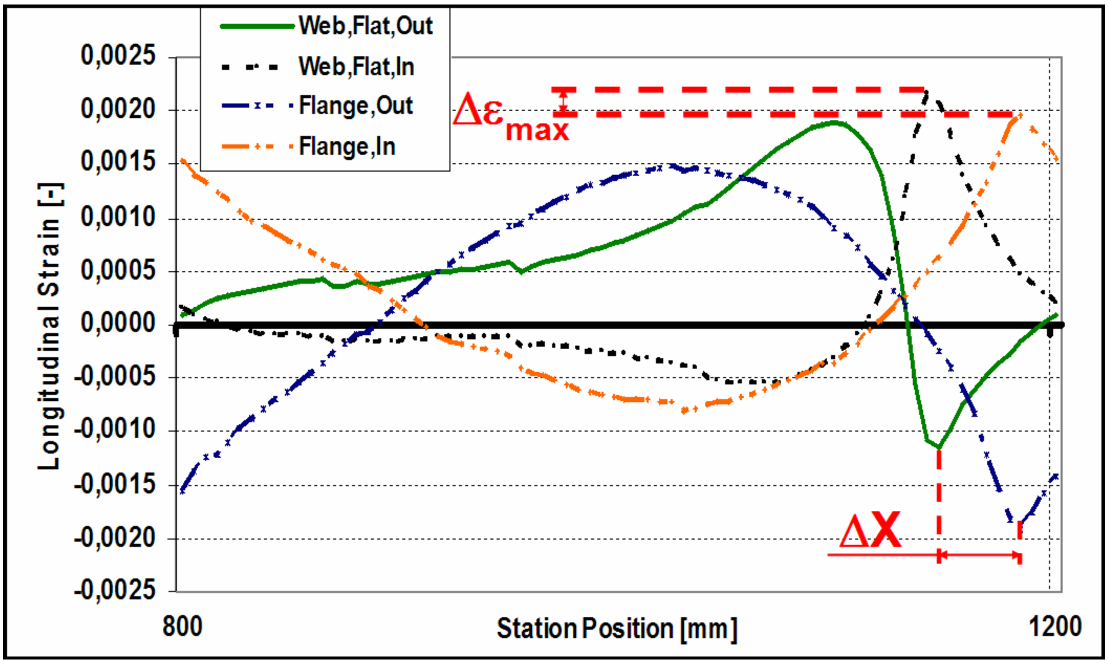

Figure 5.10: Comparison of the Longitudinal Strain Values between the 3rd and the 4th Forming Stations (WH=49mm, FL=15mm)

As Figure 5.11 clearly indicates, while the spatial flow of the flat strip in between two forming stages can be described by a sinusoidal "Shape Function", the flow of the bifurcated strip is close to linear.

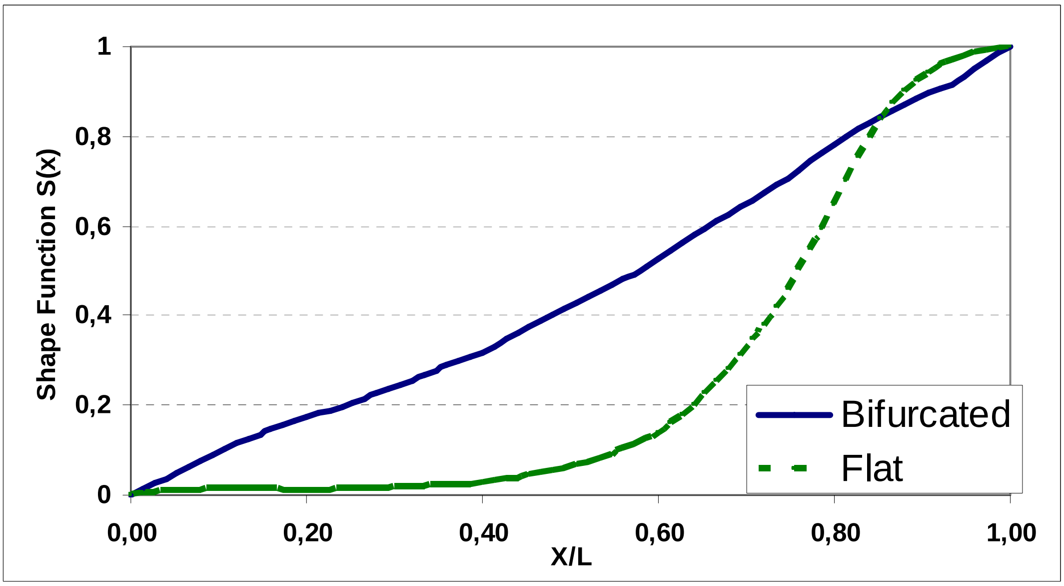

Figure 5.11: Comparison of the "Shape Functions" as Predicted using FEA (WH=49mm, FL=15mm)

6. NUMERICAL INVESTIGATION OF THE BIFURCATED PROFILE

In order to derive emprical relations for roll forming of bifurcated profiles, the basic FE model geometry of the profile will be used which is produced with the existing roll forming tool in the SFB666 hall. The existing geometry is a simple U-profile (See Fig. 4.3). The symmetrical shape of the U-profile is an advantage for the FE simulation, because by modeling only one half of the sheet, the simulation time can be reduced drastically. Another advantage of using this geometry is that FE model of this geometry is already validated by a number of experiments. Thus, expensive tooling cost for an additional experiment is saved.

As the longitudinal strain is the main criterion in designing the flower diagram by roll forming, by varying the geometrical parameters of the basic model, semy-emprical relations will be derived. In following chapters, web height, flange length and bending sequence will be varied and the effect of the variations will be inspected in comparison to basic geometry.

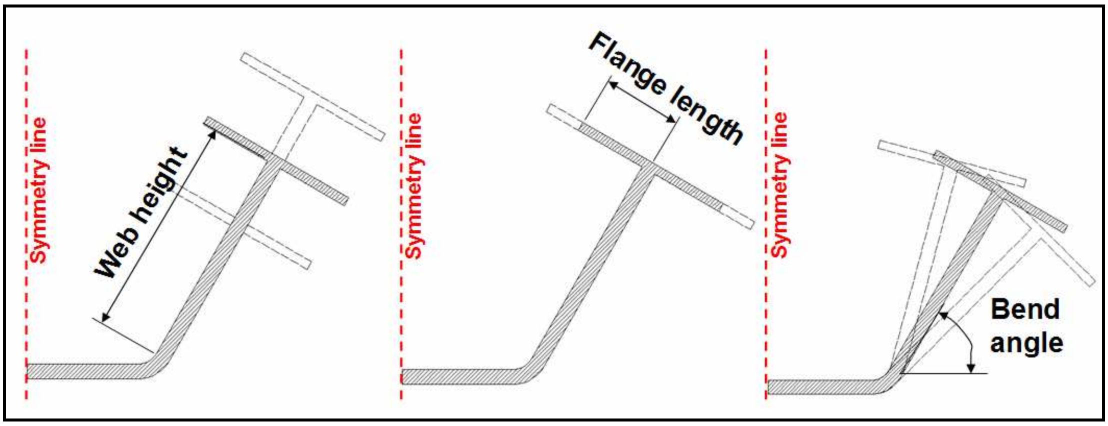

Figure 6.1: Variation Parameters

6.1 Variation of the Web Height

The first variation parameter is the web height. The basis model has a height of 49 mm. It is indicated in the following table with a dotted pattern. The web height will varied in 11 simulations with 10 mm steps starting from 19 mm.

Table 6.1: Web Height Variation Steps

Simulation No.	1	2	3	4	5	6	7	8	9	10	11
Web Height [mm]	19	29	39	49	59	69	79	89	99	109	119

The results of the simulations will be used by the definition of the maximum longitudinal strain during roll forming of bifurcated sheets.

6.1.1 The FE model

The FE models for the web height variation are generated with Python scripts. For the modeling of the rolls and the bifurcated sheet, the same concepts as in the basic model are used. By the modeling of the bifurcated sheet, the only difference between sheet models is the length of the web, namely the distance from the bending zone to the flange. As in the basic model, in the bending zone, three elements are used to generate the sheet thickness. However on the other sections of the bifurcated sheet, including the flange, only one element is used over the thickness. “Assumed Strain” formulation is used for all elements.

It is known that the web of the bifurcated sheet is prone to fracture if the profile is supported insufficiently by the bottom rolls [18]. Therefore, the roll geometries should be optimized to prevent breaking. The support surface lengths of the bottom rolls are lengthen or shorten in 10 mm steps relative to the web height of the current variation. The top roll geometries are not changed for the variations with web height longer than the basic model. But for the variations shorter than the basic model, the width of the rolls is reduced, so the sheet metal doesn’t collide with the roll side surfaces during the simulation (Fig 6.2). On the contrary to the basic model, the side rolls between the last two forming stages are not modeled.

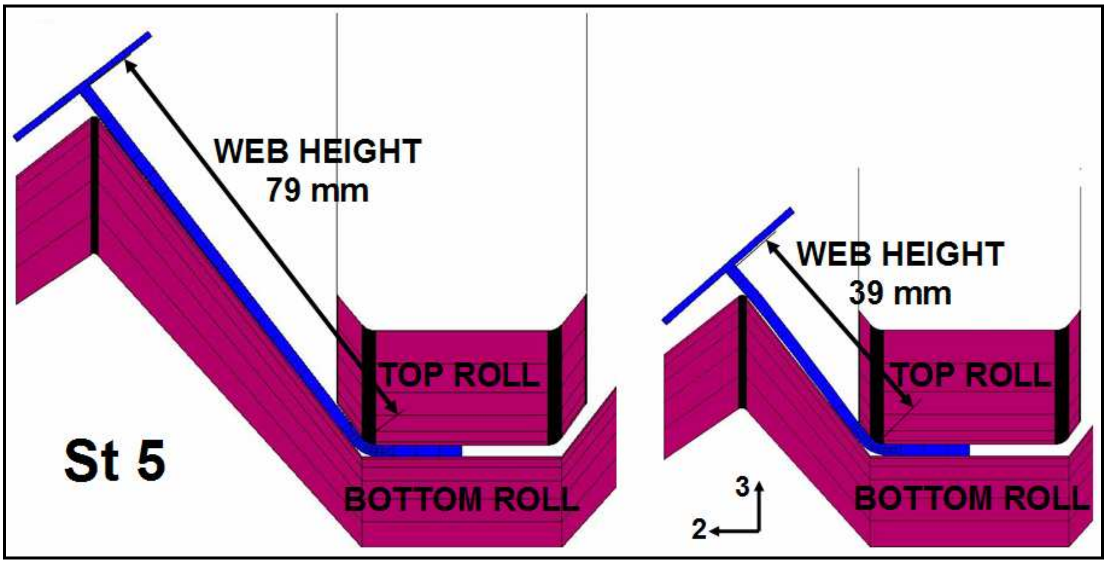

Figure 6.2: Roll Geometries of Different Variants

6.1.2 Simulation results

The results of the simulation for the web height of 19 mm will not be used to define analytical relations, because, as illustrated in the following figure, the web breaks during the simulation. This break causes longitudinal strain values which do not represent the situation of a normal web (Fig 6.3).

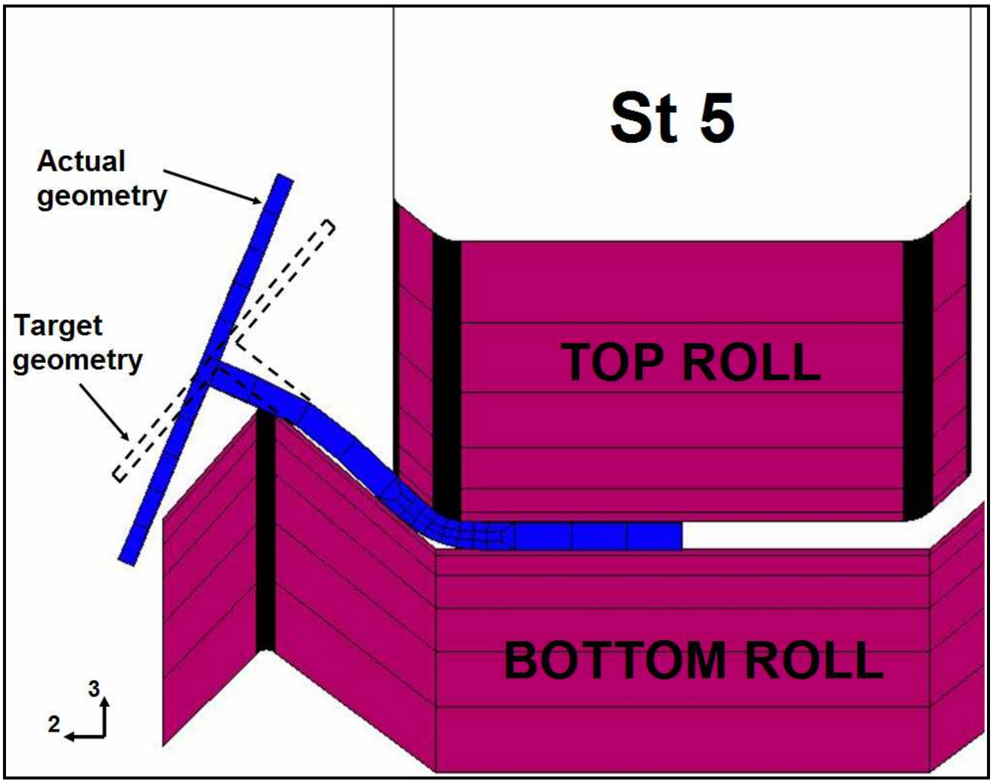

Figure 6.3: Deformed Bifurcated Sheet with a Web Height of 19 mm on the 5th Forming Stage

As indicated in the Figure 6.4, the outer edge of the flange of the variation with 29 mm web heights deforms plastically during roll forming with the current bending sequence. The plastic deformation first occurs at the second forming stage by the model with a web height of 29 mm. Here, the outer edge is pressed. Then, between the third and the fourth stage, the outer edge of the flange is elongated. Therefore, by the determination of the maximum longitudinal strain, elongation values between these forming stages will be added to the longitudinal elastic strain values to get the real longitudinal strain values. In this figure, “Elastic” and “Plastic” in the diagram key indicate the elastic and plastic strain values.

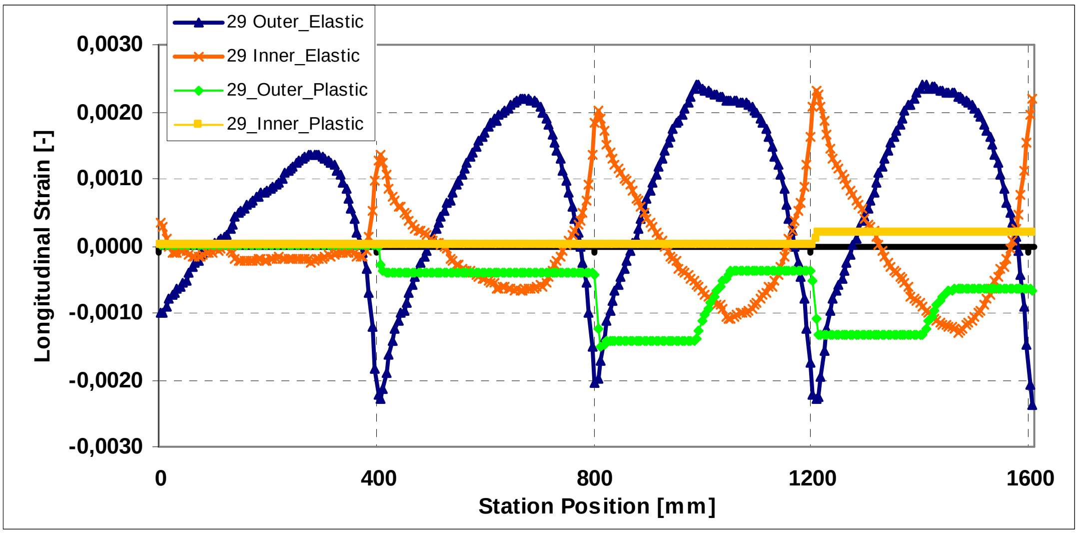

Figure 6.4: Longitudinal Strain Development by a Web Length of 29 mm

Figures 6.5, 6.6, 6.7 and 6.8 show the longitudinal strain values occurring during roll forming of bifurcated sheets with different web heights of 39, 49, 59 and 69 mm. Here, “Outer” indicates the longitudinal strain at the outer flange edge while “Inner” indicates the longitudinal strain at the inner flange edge. The numbers in the diagram key indicates the flange length of the current analyze. In the following diagrams, all the strain values are in the elastic region.

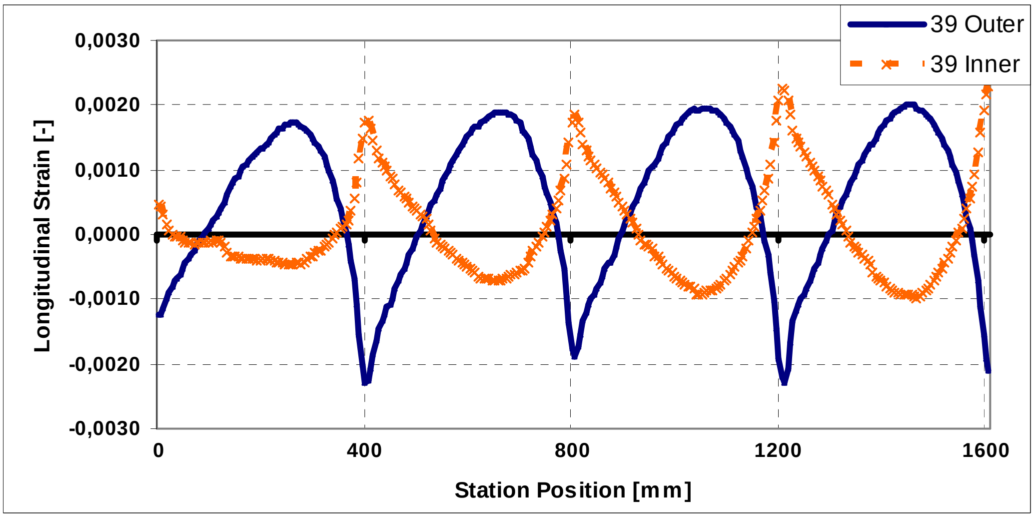

Figure 6.5: Longitudinal Strain Development by a Web Length of 39 mm

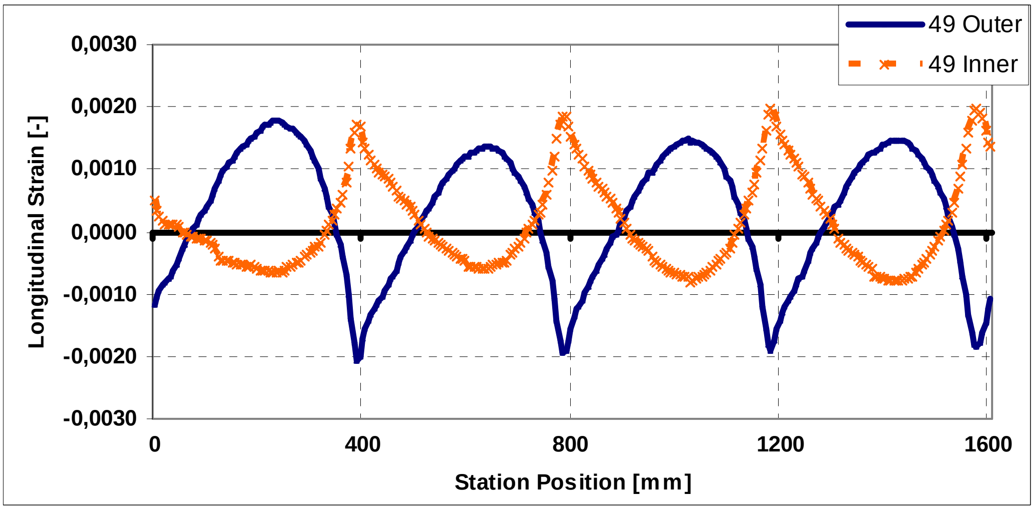

Figure 6.6: Longitudinal strain development by a web length of 49 mm

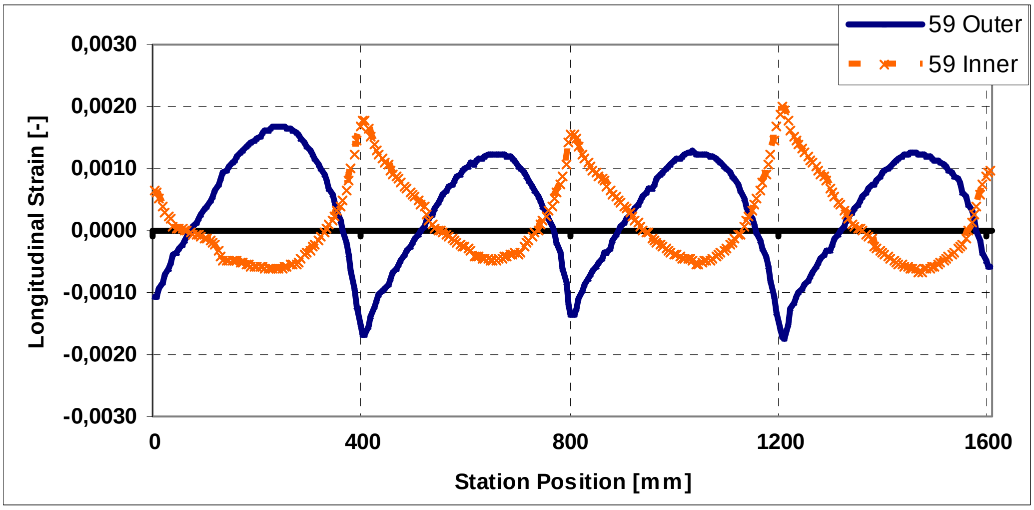

Figure 6.7: Longitudinal Strain Development by a Web Length of 59 mm

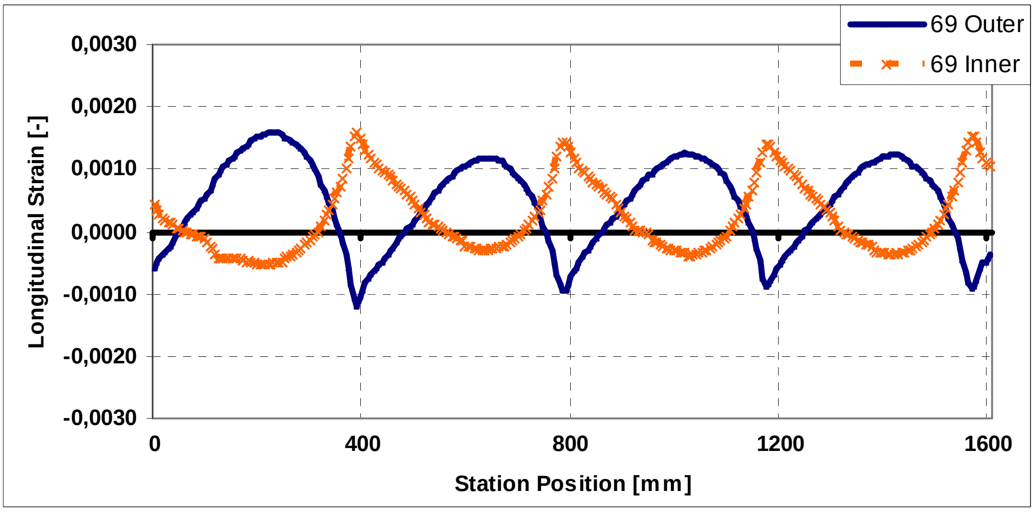

Figure 6.8: Longitudinal Strain Development by a Web Length of 69 mm

In the previous diagrams, it is highlighted that the maximum longitudinal strain values on the outer edge of the flange decreases as the web height increases. Another point is the increase in minimum longitudinal strain values on the outer edge of the flange as the web height increases. Similarly, the maximum longitudinal strain values on the inner edge of the flange decrease as the web height increases. For the minimum longitudinal strain values on the inner edge of the flange, similar observations can be made as the ones on the outer edge of the flange, namely the minimum longitudinal strain values increases as the web height increases. Till a web height of 69 mm, the values of longitudinal strain on the inner edge of the flange are higher than the ones on the outer flange edge.

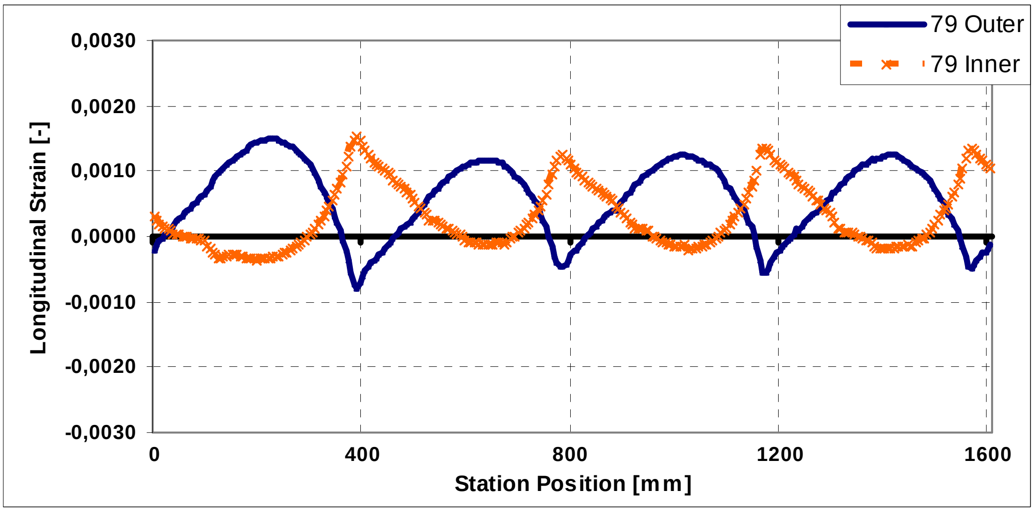

Figure 6.9: Longitudinal Strain Development by a Web Length of 79 mm

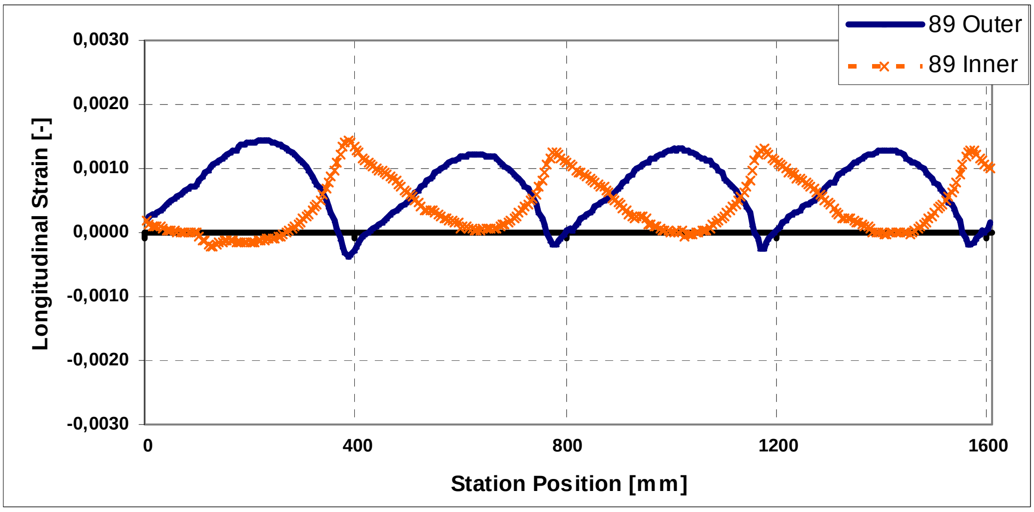

Figure 6.10: Longitudinal Strain Development by a Web Length of 89 mm

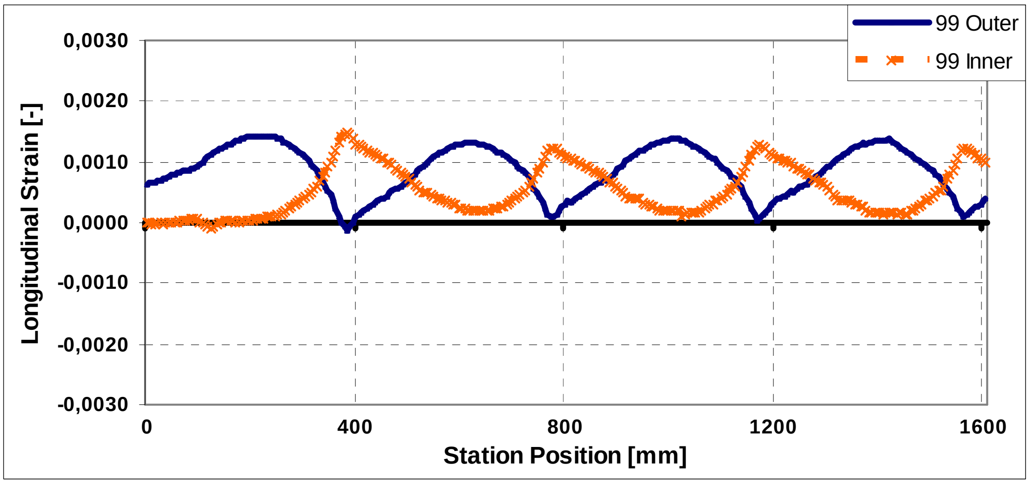

Figure 6.11: Longitudinal Strain Development by a Web Length of 99 mm

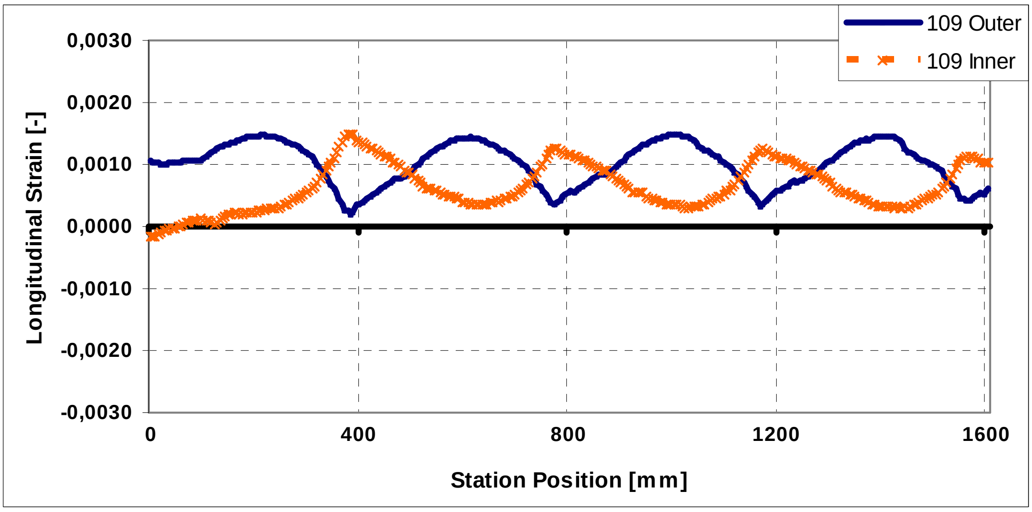

Figure 6.12: Longitudinal Strain Development by a Web Length of 109 mm

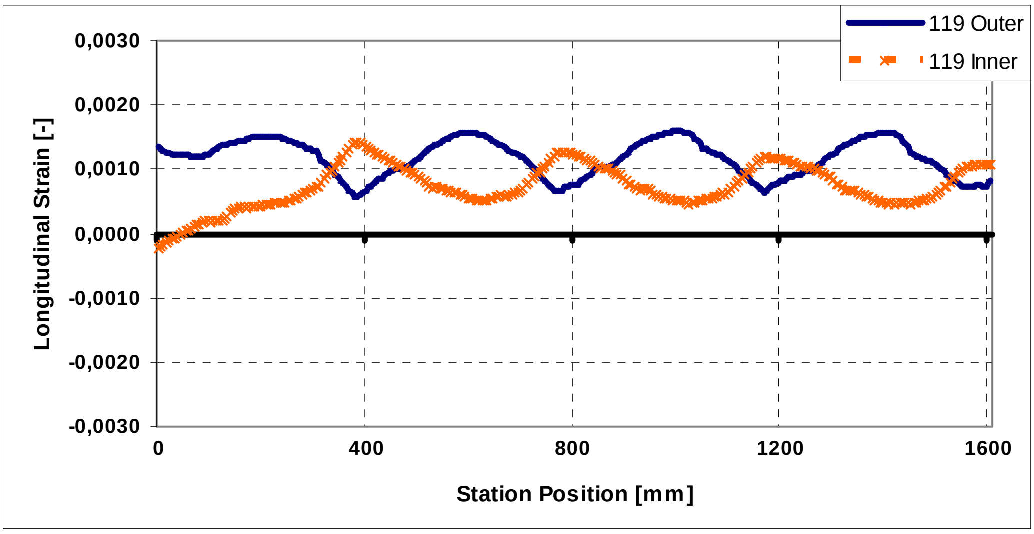

Figure 6.13: Longitudinal Strain Development by a Web Length of 119 mm

As the web height increases, the longitudinal strain values on the outer flange edge become more significant. By web heights higher than 79 mm, the maximum longitudinal strain on the outer flange is higher than the ones on the inner flange. For the values of web height higher than 89 mm, it is observed that on both, the outer edge and the inner edge of the flange the longitudinal strain values are in the elongation section.

6.1.3 Summary of the web height variation results

The bifurcated profile will not be bent with equal angles during the real process, and so during the simulation. The bending starts with an 8^0 step and continues with seven 11^0 steps (See Table 5.1). It is known that, if the bending angle changes during a roll forming process, a quick rise in the longitudinal strain values are expected at the first forming station with the different angle [17]. The main goal is the definition of the emprical relations during roll forming of the bifurcated profiles first for a basic system. Therefore, the longitudinal strain values between 1st and the 2nd forming stations will not be used by the analytical relations definition.

Following figure shows the maximum elongation strain values occurring during roll forming of the bifurcated sheets with different web heights. The basis model, namely the one with a web height of 49 mm, is indicated in the column with a squared pattern. As seen in Figure 6.14, the maximum longitudinal strain values increase drastically while the web height decreases. After reaching a minimum value, these values start to increase again.

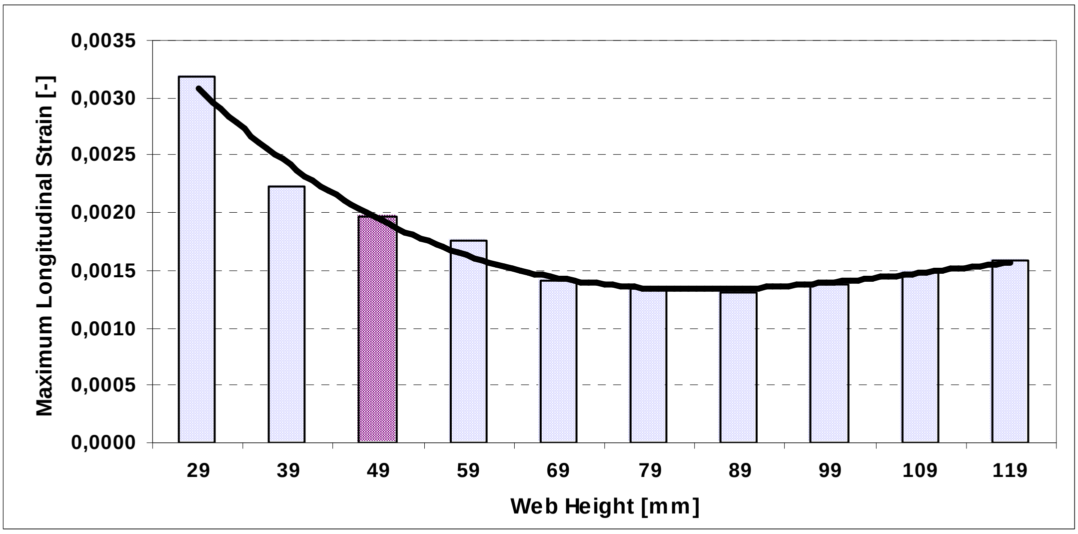

Figure 6.14: Maximum Longitudinal Strain at the Flange Edge

6.2 Variation of the Flange Length

The second variation parameter is the flange length. As starting model, basis model with a web height of 49 mm and a flange length of 15 mm will be used. It is indicated in the following table with a dotted pattern. The web height will varied in 5 simulations with 5 mm steps starting from 5 mm

Table 6.2: Flange Length Variation Steps

Simulation No.	1	2	3	4	5
Flange Length [mm]	**5**	**10**	**15**	**20**	**25**

6.2.1 The FE model

On this variant, the starting model is the same as in the basis model. Roll geometries of the basis model will also be used for the variants with flange lengths lower than the basis model. But for the ones with higher flange lengths, the roll geometries have to be change to prevent collision between sheet and the roll. Therefore, the width of the rolls is adapted to the new flange geometry.

As for the bifurcated sheet model, the geometry is the same as the basis model except the flange section. Therefore, the only variation by the bifurcated sheet model is the flange length, namely the element numbers on the flange section.

6.2.2 Simulation results

Following figures show the longitudinal strain values occurring during roll forming of bifurcated sheets with different flange lengths. Here, "Outer" indicates the longitudinal strain at the outer flange edge while "Inner" indicates the longitudinal strain at the inner flange edge. The numbers staring with an "F" indicates the flange length of the current analyze.

As shown in the Figure 6.15 and 6.16, the outer and inner edge of the flange deforms plastically if the current bending sequence is used.

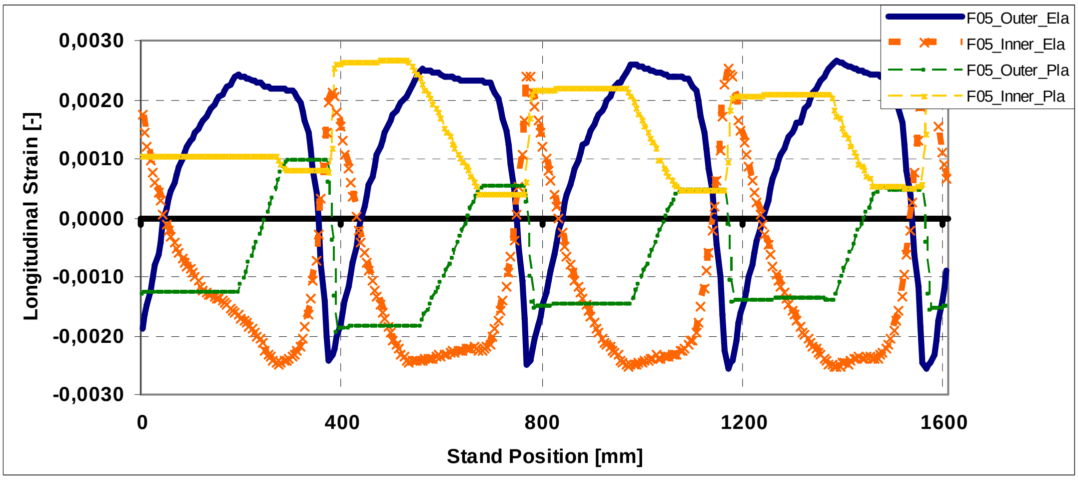

Figure 6.15: Longitudinal Strain Development by a Flange Length of 5 mm

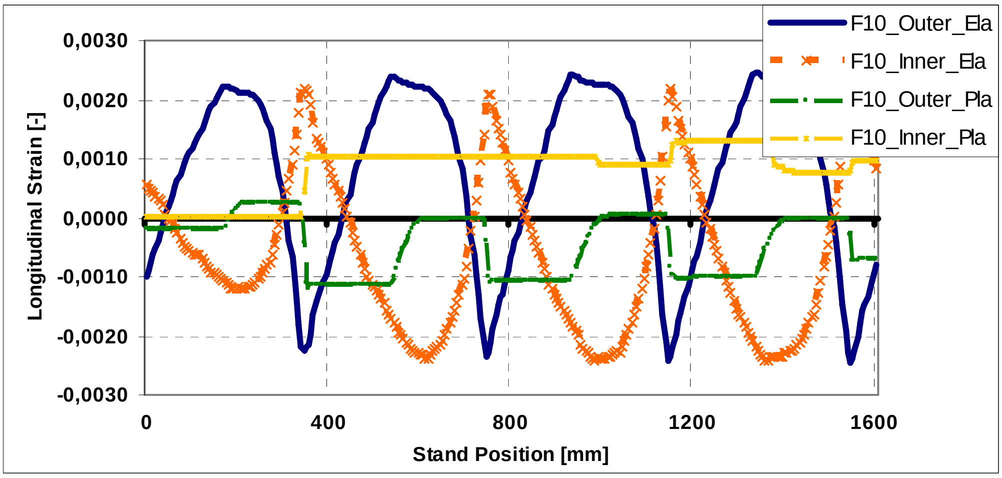

Figure 6.16: Longitudinal Strain Development by a Flange Length of 10 mm

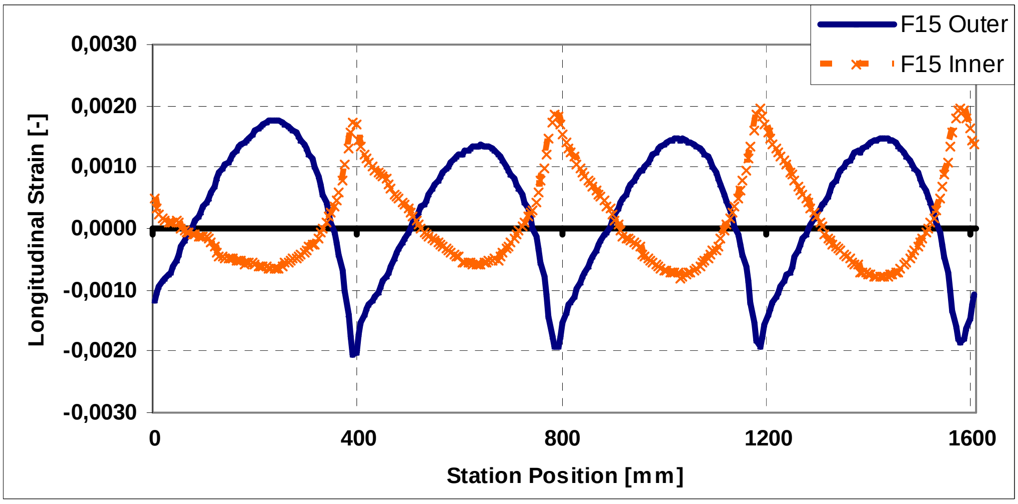

Figure 6.17: Longitudinal Strain Development by a Flange Length of 15 mm

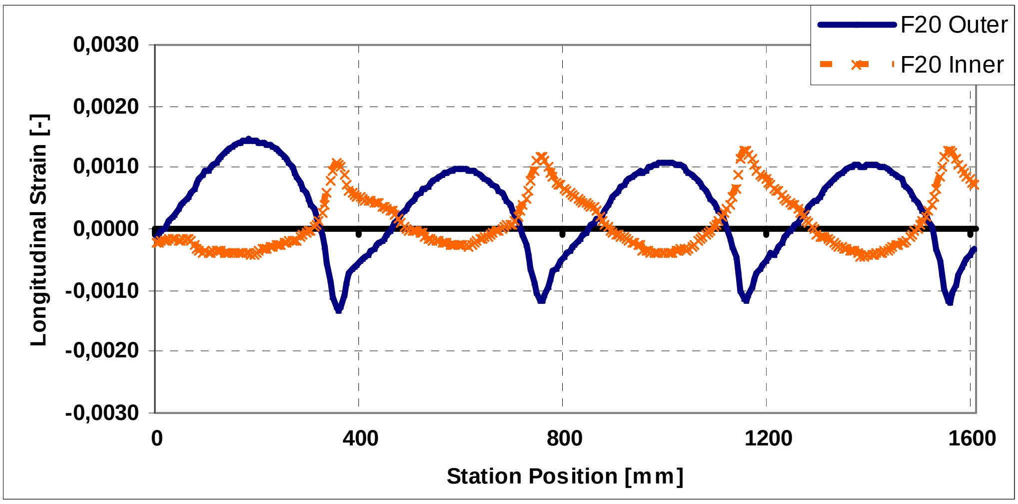

Figure 6.18: Longitudinal Strain Development by a Flange Length of 20 mm

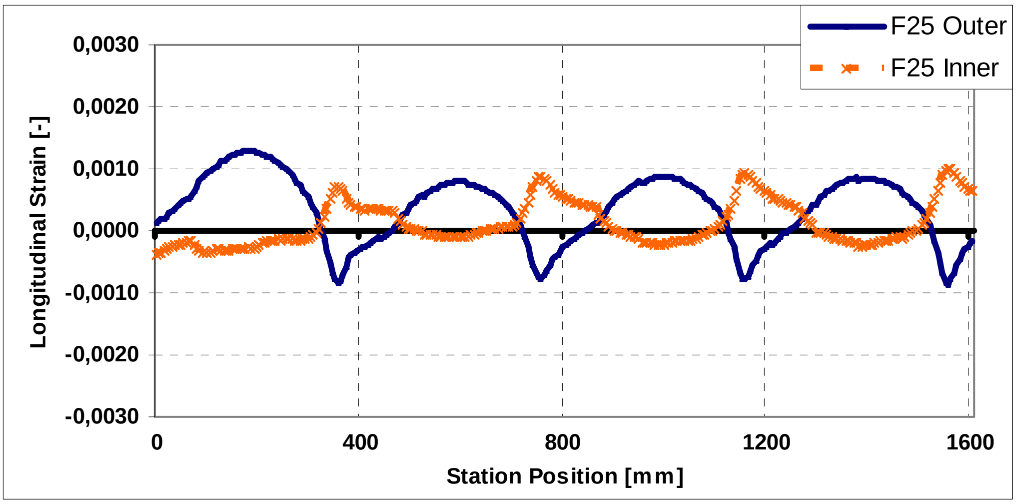

Figure 6.19: Longitudinal Strain Development by a Flange Length of 25 mm

6.2.3 Summary of the flange length variation results

As mentioned in the previous section, the strain values between the 1st and the 2nd forming stations will not be analyzed. The figures 6.15 and 6.16 indicates the longitudinal elastic and plastic deformation during roll forming of the bifurcated sheet with a flange length of 5 mm and 10 mm. As it can be seen in these figures, the flange outer and inner edges deform plastically during roll forming. Therefore, by the determination of the maximum longitudinal strain, the plastic strain change is added to the elastic strain values to get the real longitudinal strain values.

Figure 6.20 shows the maximum elongation strain values occurring during roll forming of the bifurcated sheets with different flange lengths. The basis model, namely the one with a flange length of 15 mm, is indicated in the column with a squared pattern.

The maximum values decreases while the flange length increases. The results of the simulations show the same trend with the outcome of previous studies [18].

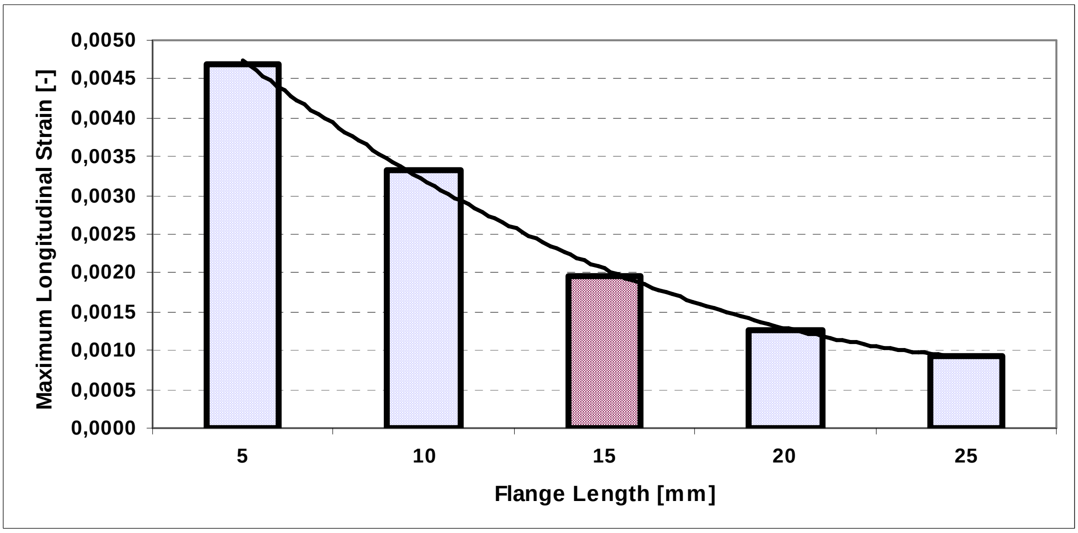

Figure 6.20: Maximum Longitudinal Strain at the Flange Edge

6.3 Variation of the Bending Angle

The third and the last variation parameter is the bending angle. The basis model for the FE simulations is the same as in the other variations. But the bending sequence differ form other variants, even from the basis model. To provide equality between longitudinal strain values occurring during roll forming, the bending sequences with regular bending angles are selected. Following table indicates the three variants and their bending angles, forming step numbers and total bend angles. The bending angle with the dotted pattern in the table above corresponds to the basis model. However, in the basis model, bending starts with an angle of 8^0 and continues with 11^0 steps. However in the variations, the bending angle does not change in between stations. As in the web height and flange length variations, longitudinal strain conditions will be analyzed after the 1st forming stage.

Table 6.3: Bending Angle Variation Parameters

Variant	1	2	3
Bending Angle	8	11	14
Step Number	9	8	6
Total Bend Angle	72	88	84

6.3.1 FE model

In all bending angle variations, the same sheet model as the basis model will be used. Since the bending sequence and so the roll geometries differ from the existing the ones in the existing process, new tool geometries have to be designed for all variants. These tools are designed with the program COPRA RF. Instead of exporting the geometries directly to the FE analyze program MARC/Mentat, the cross section geometries of the rolls are read from the program COPRA RF and using these coordinates, FE models of the rolls are generated via a Python script. All the FE related parameters are defined also with this script. The main advantage of this approach is by doing so; it is assured that the generated geometries and the models have the same properties as the other variation models. The main difference of the bending sequence variation model from the other ones is the intermediate idler rolls between the last two forming stages, because these rolls are not included in these simulations.

In the bending sequence variation models, the increment size is adapted to the number of forming stages, namely to the forming length. By the definition, the increment size which corresponds to 1.075 mm roll movement is implemented.

6.3.2 Simulation results

Figures 6.21, 6.22 and 6.23 show the longitudinal strain values occurring during roll forming of bifurcated sheets with different bending sequences. Here, "Outer" indicates the longitudinal strain at the outer flange edge while "Inner" indicates the longitudinal strain at the inner flange edge. The numbers in the key indicate the bending angle of the current analyze.

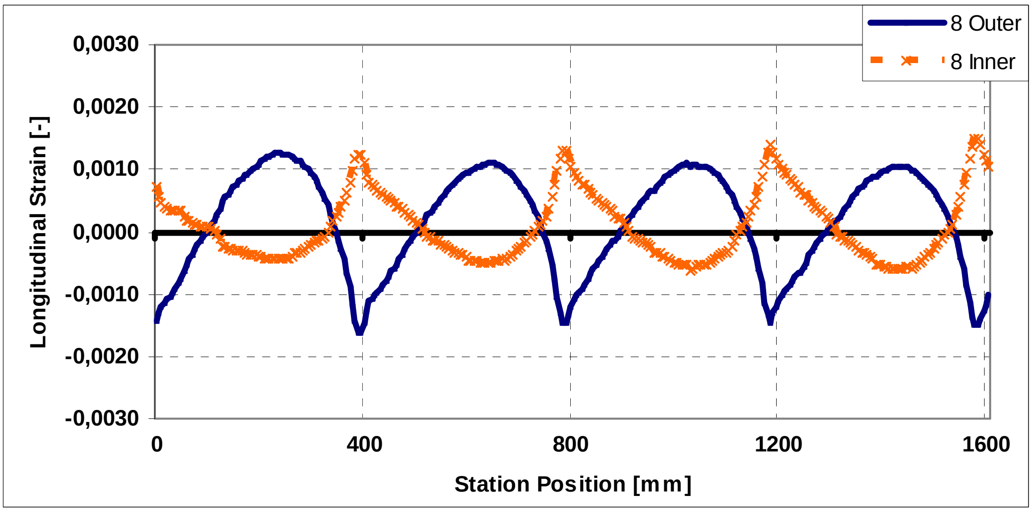

Figure 6.21: Longitudinal Strain Development by a Bending Sequence with 8^0

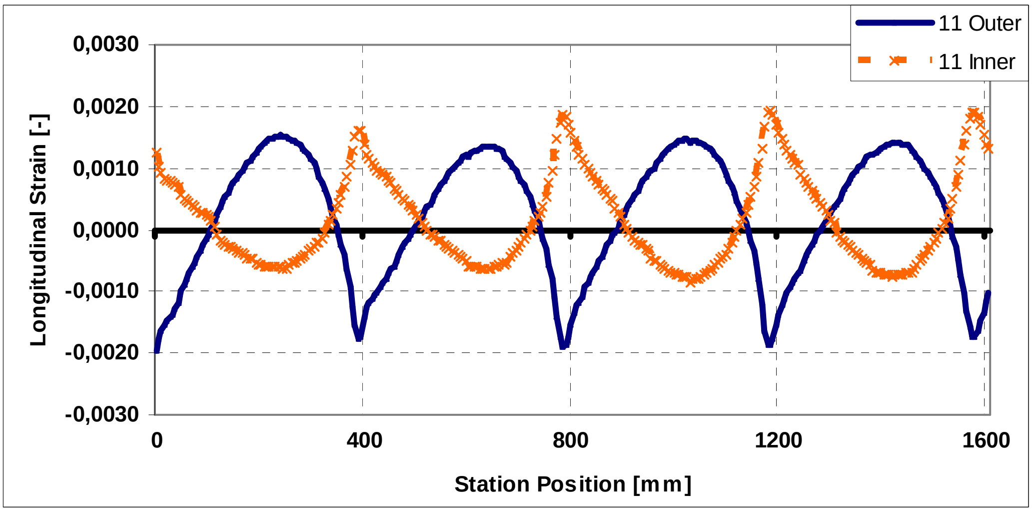

Figure 6.22: Longitudinal Strain Development by a Bending Sequence with 11^0

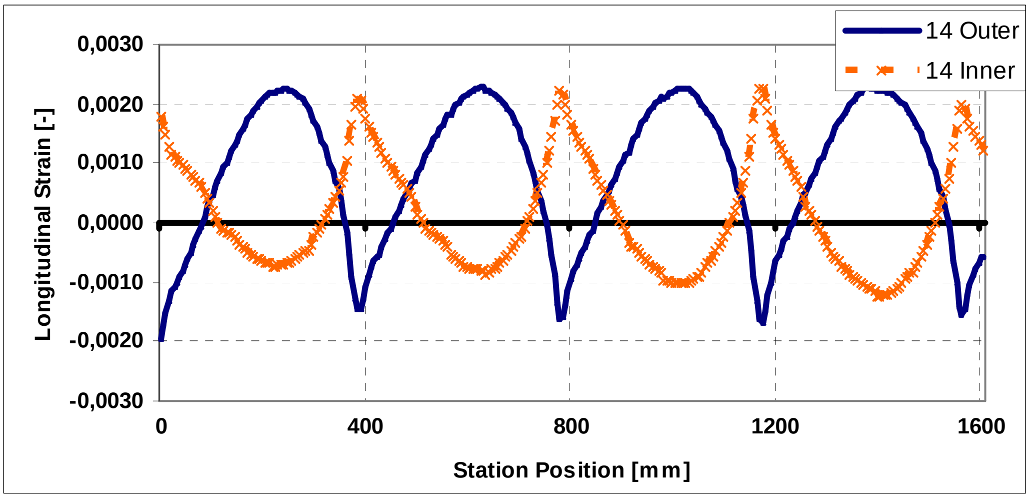

Figure 6.23: Longitudinal Strain Development by a Bending Sequence with 14^0

6.3.3 Summary of the bending sequence variation results

Figure 6.24 shows the maximum elongation strain values occurring during roll forming of the bifurcated sheets with different bending sequences. The bending sequence which corresponds to the basis model is indicated in the column with a squared pattern. As seen above, the maximum longitudinal strain values increase while the bending angle increases. The correlation is close to linear.

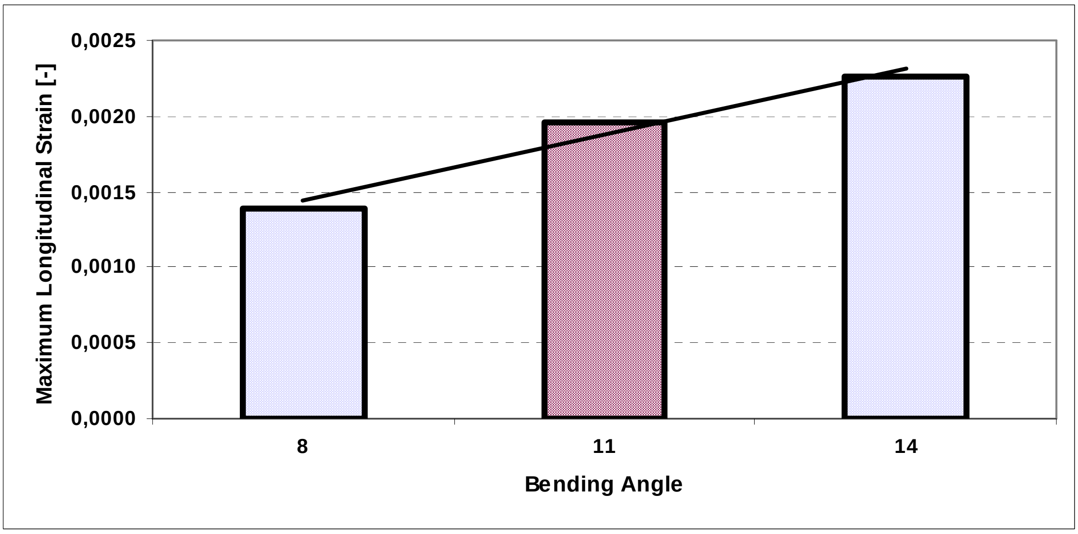

Figure 6.24: Maximum Longitudinal Strain at the Flange Edge

6.4 Analytical Definition of the Maximum Longitudinal Strain

Over the years, different concepts have been developed to define the longitudinal strain development in flat sheets during roll forming (See Chapter 2.1.4.). There are several software packages in the market to analyze the strain conditions occurring during roll forming (See Chapter 2.1.5).

However, up till now, the processing of integral bifurcated profiles in a roll forming line is not apprehended analytically. In this chapter, an analytical formula will be derived for the maximum longitudinal strain occurring during roll forming of the bifurcated profiles relative to the web height, flange length and bending angle. To derive the formula, the results of the variation simulations will be used.

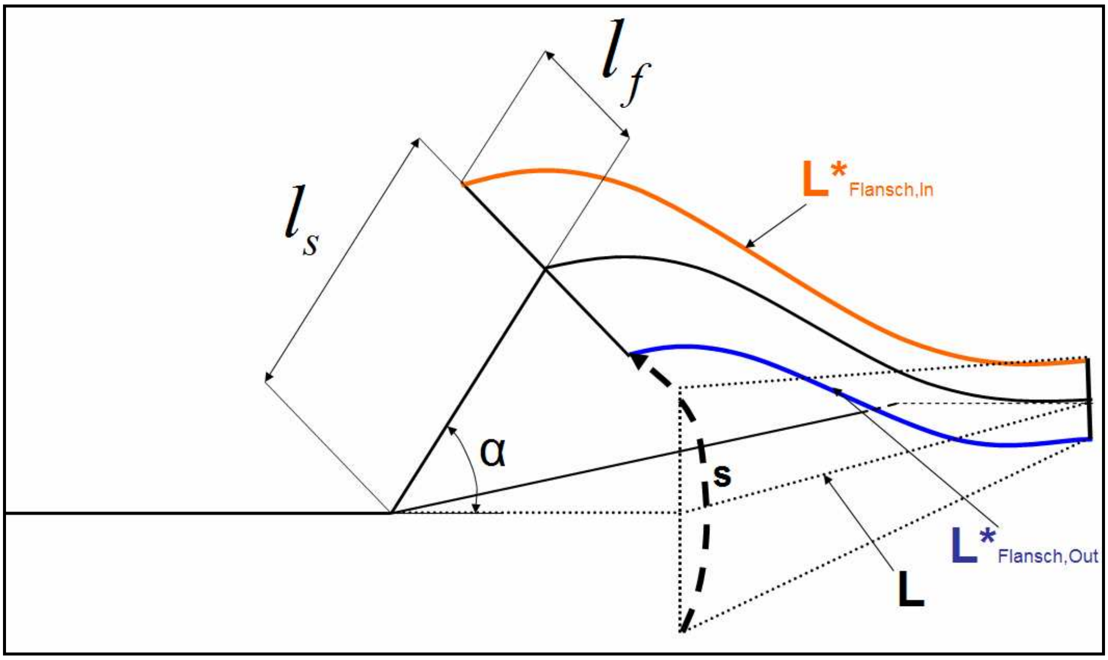

Figure 6.25: Schematic representation of the bifurcated sheet travel during roll forming

By the derivation of the formula, a linear approach will be implemented. By linear approach, there is no difference by the travel denoted by $L*_{Flansch,Out}$ and $L*_{Flansch;In}$ because the distance between the starting position and the end position of the edge point of the outer flange is equal to the distance between the starting position and the end position of the edge point of the inner flange. Therefore, the travel both edge of the flanges will be denoted as $L*$.

While the bend line travels a straight line during forming, the bend edge, namely the flange edge travels in a helical pattern. The length of this travel is calculated as follows:

$$L^* = \sqrt{L^2 + s^2} \qquad \textbf{(6.1)}$$

where L is the length of the bending line which is equal to the distance between two consecutive forming stations and s is the circular path of the flanges end point during forming.

The s length can be described as follows.

$$s = \sqrt{{l_s}^2 + {l_f}^2} \cdot \theta \qquad \textbf{(6.2)}$$

Here, l_s is the web height; l_f is the flange length and θ is the bending angle in radian. Therefore, formula 6.1 can be expressed as

$$L^* = \sqrt{L^2 + [({l_s}^2 + {l_f}^2) \cdot \theta^2]} \qquad \textbf{(6.3)}$$

The maximum longitudinal strain values occurring during roll forming of bifurcated profiles are not directly proportional to the web height, flange length and bending angle. This indicates a difference by the length of the travel of the bend edge between calculated values and values obtained from the simulations. Therefore, to fit the longitudinal strain values calculated with the above formula to the longitudinal strain values which are obtained from the simulations, correction factors has to be defined. Therefore, the Equation 6.3 becomes:

$$L^* = k_s \cdot k_f \cdot k_\theta \cdot \sqrt{L^2 + [({l_s}^2 + {l_f}^2) \cdot \theta^2]} \qquad \textbf{(6.4)}$$

Here, k_s is the web height correction factor, k_f is the flange length correction factor and k_θ is the bending angle correction factor.

In this study, the effects of the web thickness and flange thickness will be neglected. The correction factor will be defined for the steel H480 LA. The web thickness is taken as 2 mm and flange thickness as 1.2 mm. Since the effects of the distance between two consecutive forming stations on the longitudinal strain are not investigated, the correction factors are defined for a inter station distance of 400 mm.

The main approach by the definition of the correction factors is to calculate the length of the travel of the bend edge between two consecutive forming stages and than comparing it with the values obtained from simulations. The correction factors are mainly the ratio of these two values. Following diagram shows the ratio of the calculated maximum longitudinal strain values to the values obtained from the web height variation simulations.

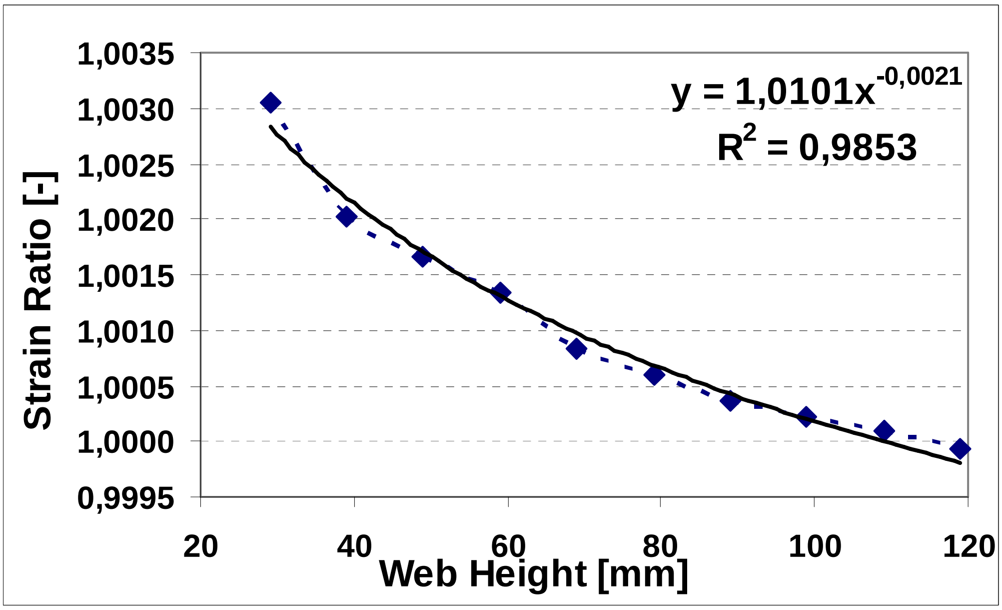

Figure 6.26: Ratio of the Calculated and Simulated Strain Values

The equation of the fitting curve in the figure above mainly builds the web height correction factor. It can be described as follows.

$$k_s = 1{,}0101 \cdot l_s^{-0{,}0021} \tag{6.5}$$

In order to describe the bending angle correction factor, maximum longitudinal strain values calculated with the Equation 6.3 by using the web height correction factor will be compared with the values obtained from the bending angle variation simulations. The following diagram shows the ratio of the calculated maximum longitudinal strain values to the values obtained from the bending angle variation simulations.

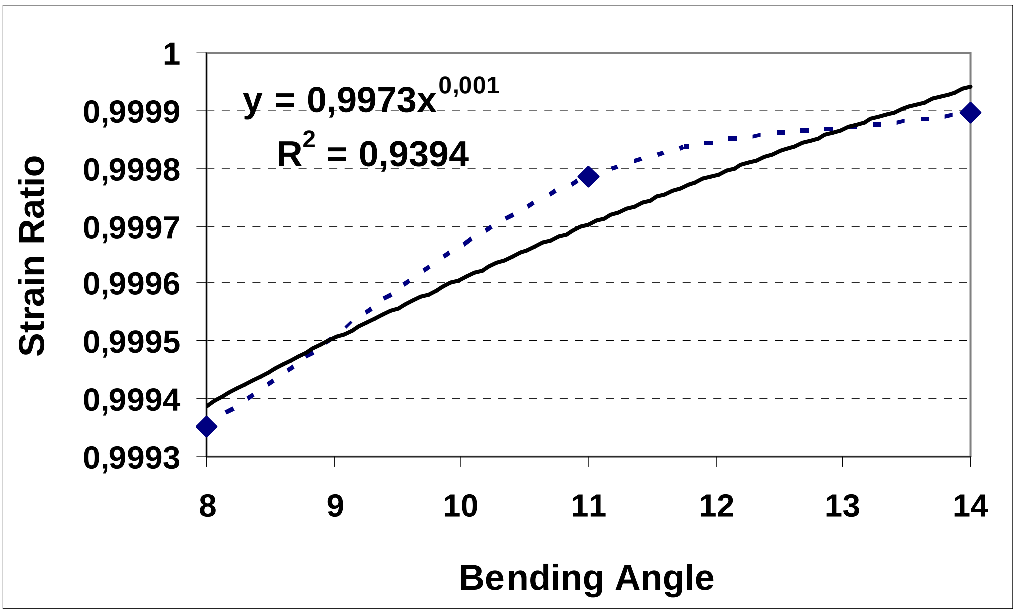

Figure 6.27: Ratio of the Calculated and Simulated Strain Values

The equation of the fitting curve in the figure above mainly builds the bending angle correction factor. It can be described as follows.

$$k_\theta = 0{,}9973 \cdot \theta^{0{,}001} \quad \textbf{(6.6)}$$

In order to describe the flange length correction factor, maximum longitudinal strain values calculated with the Equation 6.3 by using the web height and bending angle correction factors will be compared with the values obtained from the flange length variation simulations. The following diagram shows the ratio of the calculated maximum longitudinal strain values to the values obtained from the flange length variation simulations.

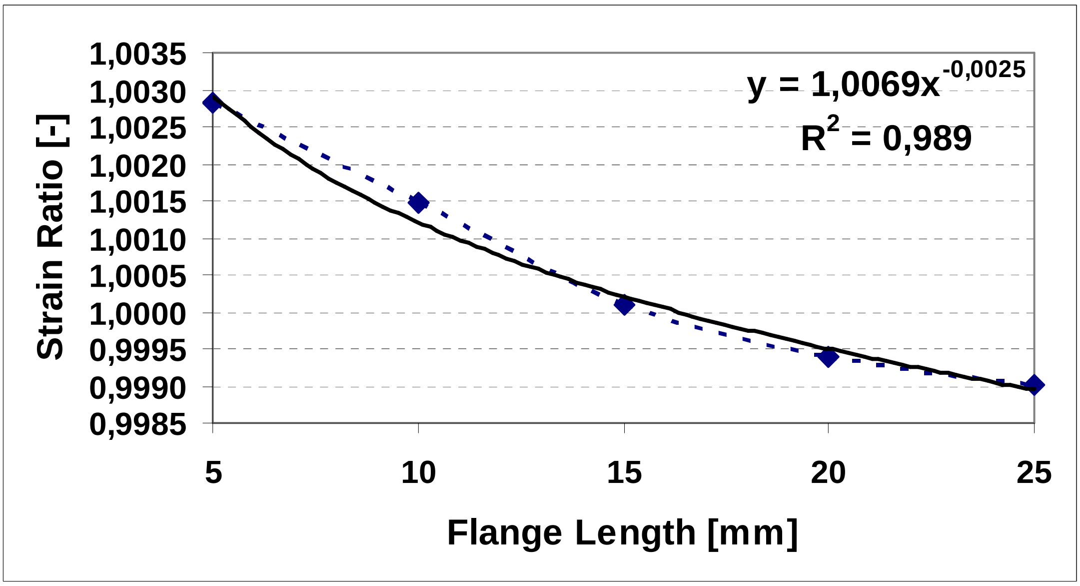

Figure 6.28: Ratio of the Calculated and Simulated Strain Values

The equation of the fitting curve in the figure above mainly builds the bending angle correction factor. It can be described as follows.

$$k_f = 1{,}0069 \cdot l_f^{-0{,}0025} \tag{6.7}$$

By putting the correction factors into Equation 6.4, it reduces to

$$L^* = 1{,}01432 \cdot l_s^{-0{,}0021} \cdot l_f^{-0{,}0025} \cdot \theta^{0{,}001} \sqrt{L^2 + [(l_s^2 + l_f^2) \cdot \theta^2]} \tag{6.8}$$

Finally, the maximum longitudinal strain values can be calculated by entering the band edge length values to the following equation:

$$\varepsilon = \frac{L^* - L}{L} \tag{6.9}$$

Maximum longitudinal values calculated with the Equation 6.7 deviates form the ones obtained from the simulations. The deviation rates are shown in the Tables 6.4, 6.5 and 6.6. In these tables, variation parameters which correspond to the basis model are indicated with a dotted pattern. The highest deviation with 20.2 % is observed by a web height of 49 mm, a flange length of 25 mm and a bending angle of 11^0. Other than that, the deviation values are under 10.4 %.

Table 6.4: Deviation of Calculated Maximum Longitudinal Strain Values from the Ones Obtained from Web Height Variation Simulations

Web Height [mm]	Max. Long.Strain (Simulation)	Max. Long. Strain (Calculation)	Deviation [%]
29	0,00318	0,00291	-8,6
39	0,00223	0,00236	5,8
49	0,00196	0,00198	0,9
59	0,00176	0,00172	-2,6
69	0,00141	0,00153	8,7
79	0,00135	0,00142	5,2
89	0,00131	0,00136	4,0
99	0,00138	0,00135	-1,8
109	0,00148	0,00139	-6,0
119	0,00158	0,00147	-7,0

Table 6.5: Deviation of Calculated Maximum Longitudinal Strain Values from the Ones Obtained from Flange Length Variation Simulations

Flange Length [mm]	Max. Long.Strain (Simulation)	Max. Long. Strain (Calculation)	Deviation [%]
5	0,00468	0,00471	0,7
10	0,00333	0,00298	-10,4
15	0,00196	0,00198	0,9
20	0,00127	0,00128	0,5
25	0,00094	0,00075	-20,2

Table 6.6: Deviation of Calculated Maximum Longitudinal Strain Values from the Ones Obtained from Bending Angle Variation Simulations

Bending Angle	Max. Long.Strain (Simulation)	Max. Long. Strain (Calculation)	Deviation [%]
8	0,00139	0,00152	9,3
11	0,00196	0,00198	0,9
14	0,00226	0,00241	6,5

7. CONCLUSIONS

Because of its high flexibility and productivity, roll forming has developed as one of the most important forming methods. With this method, many profiles varying in their shape, materials, thickness, etc. can be produced. The new production method, linear flow splitting enlarges the range of the semi finished products which can be used in roll forming. With the utilization of the splitted profiles in roll forming, the product spectrum of this forming method can be enlarged.

The definition of the analytical relations during roll forming of bifurcated profiles creates the basis of this study. The longitudinal strain occurring during roll forming of the bifurcated profiles is the center of the investigations. During the studies, an FE approach will be implemented. The parameters such as web height, flange length and bending angle will be varied in predefined steps. The maximum strain occurring during roll forming in longitudinal direction will be analyzed.

Since the goal of this study is to define analytical relations during roll forming of bifurcated profiles using FE simulations, the necessity to validate these simulations arises. Experiments showed that a meshing concept with 3 elements over the thickness in the FE model of the sheet metal can represent the real process with a deviation of 1.5%.

Evaluating the results of the finite element simulations conducted, general statements about the longitudinal strain development during roll forming of bifurcated profiles can be made. The longitudinal strain values have a minimum depending on the web height. The reduction of the web height under this level or the increase of it above this level causes an increase in the strain values. The reduction of the bending angle has a positive effect on the longitudinal strain values, namely the strain values decreases as the bending angle decreases. On the contrary, the strain values decrease while the flange length increases. A semi-emprical formula has been defined by using the linear approach to calculate the maximum longitudinal strain occurring during roll forming of the bifurcated profiles depending on the web height, flange length and bending angle. However, the formula deviate from the maximum longitudinal strain values obtained from the simulations. The highest deviation with 20.2 % is observed by a web height of 49 mm, a flange length of 25 mm and a bending angle of 11^0. Other than that, the deviation values are under 10.4 %.

In order to validate the derived formula for the maximum longitudinal strain, roll forming process of other product geometries have to be simulated. Additionally, up till now, the effect of the bifurcated sheet thickness is not analyzed. Therefore, variation of the sheet thickness and sheet material would be useful. A further step could be the investigation of the springback of the bifurcated sheet after roll forming.

REFERENCES

[1] **DIN-8582,** 2003. Fertigungsverfahren Umformen – Einordnung; Unterteilung, Begriffe, Alphabetische Übersicht, *German Institute for Standardization*, Berlin.

[2] **Altan, T. (ed),** 1998. Metal forming handbook / Schuler, Springer–Verlag, Berlin.

[3] **DIN-8586,** 2003. Fertigungsverfahren Biegeumformen – Einordnung, Unterteilung, Begriffe, *German Institute for Standardization*, Berlin.

[4] **Halmos, G.T. (ed),** 2006. Roll Forming Handbook, CRC Press, Boca Raton.

[5] **Lange, K.,** 1990, Umformtechnik-Handbuch für Industrie und Wissenschaft Band:3 Blechbearbeitung, Springer-Verlag, Berlin.

[6] **Jansen AG.** 2008. *spezgewalzt* [online]. [Accessed 3rd March 2008]. Available from world wide web: <http://www.jansen.com/e/index_s.html>

[7] **Zettler, A.O.,** 2007. Grundlagen und Auslegungs Methdoden für flexible Profilierprozesse, *Dr.-Ing. Dissertation*, TU Darmstadt, PtU, Darmstadt.

[8] **Bhattacharyya, D., Smith, P.D., Yee, C.H. and Collins, I.F.,** 1984. The prediction of deformation length in cold roll forming, *Journal of Mechanical Working Technology*, **9**, 181-191.

[9] **Kiuchi, M., Abe. K. and Onodera. R.,** 1995. Computerized Numerical Simulation of Roll-Forming Process, *CIRP Annals-Manufacturing Technology*, **41-1**, 239-242.

[10] **Groche, P., Vucic, D. and Jöckel, M.,** 2007. Basics of linear flow splitting, *Journal of Materials Processing Technology*, **183**, 249-255.

[11] **Tilman, B.,** 2006. Vergleich zweier Methoden zur Bestimmung lokaler Umformgrade verzweigten Blechstrukturen, *Dipl. Ing. Thesis*, TU Damrstadt, PhM, Darmstadt.

[12] **MSC.Marc Product Documentation,** 2005. MSC.Marc Mentat User's Guide, Version 2005r2. MSC Software Corporation.

[13] **Behring, D., Galanulis, K., Friebe, H. and Klein, M.,** 2004. Forming Analysis by ARGUS for Simulations Verification and Evaluation of Stamping Process, [Accessed 2nd April 2008]. Available from world wide web <http://www.gom.com/CONTAINER/files/simulation_varification_en.pdf>.

[14] **Tehrani, M.S., Naeini, H.M., Hartley, P. and Khademizadeh, H.,** 2006. Localized edge buckling in cold roll-forming of circular tube section, *Journal of Materials Processing Technology*, **177**, 617-620.

[15] **Lindgren, M.,** 2007. Cold roll forming of a U-channel made of high strength steel, *Journal of Materials Processing Technology*, **186**, 77-81.

[16] **MSC.Marc Product Documentation,** 2005. MSC.Marc Mentat Volume B: Element Library, Version 2005r2. MSC Software Corporation.

[17] **Damm, K.,** 1989. Ermittlung von Laengsformaenderungen beim Walzprofilieren von Standardprofilen auf einer mehrgerüstigen Anlage, *Dr.Ing. Dissertation*, TU Darmstadt, PtU, Darmstadt.

[18] **Berner, S.,** 2006. Numerische Untersuchungen neuartiger Werkzeugsystemen für die Weiterverarbeitung von Spaltprofilen, *Dipl.-Ing. Thesis*, TU Darmstadt, PtW, Darmstadt.

APPENDIX

A. PYTHON Script for the modeling of the bifurcated profile

```
from py_mentat import *

def modellAufbau(t,b,l,a,t_f):

        py_send("*job_class mechanical")
        py_send("*job_option dimen:three")
        #py_send("*exec_default_procedure set_job_default_parameter_3d_m")

        ########################################################
        #                     MESH GENERATION
        ########################################################

        py_send("*add_nodes")
        py_send("0,0,0")
        py_send("0,0,%f" % (t))
        py_send("0,%f,%f" % (y_el,t))
        py_send("0,%f,0" % (y_el))
        py_send("*add_elements")
        py_send("3,4,1,2")
        py_send("*set_duplicate_translations")
        py_send("0,%f,0" % (y_el))
        py_send("*set_duplicate_repetitions")
        nr_elem_breite = 3
        py_send("%f" % (nr_elem_breite-1))
        py_send("*duplicate_elements")
        py_send("all_existing")
        py_send("*sweep_nodes")
        py_send("all_existing")

        py_send("*add_nodes")
        py_send("0,12,0")
        py_send("0,12,2")
        py_send("0,14,2")
        py_send("0,14,0")
        py_send("*add_elements")
        max_nodes_id = py_get_int("max_node_id()")
        py_send("%f,%f,%f,%f"          %          (max_nodes_id-1,max_nodes_id,max_nodes_id-
3,max_nodes_id-2))
         py_send("*set_duplicate_translations")
        py_send("0,2,0")
        py_send("*set_duplicate_repetitions")
        py_send("4")
        py_send("*duplicate_elements")
        max_elements_id = py_get_int("max_element_id()")
        py_send("%f" % (max_elements_id))
        py_send("#")
        py_send("*sweep_nodes")
        py_send("all_existing")
```

```
        py_send("*add_nodes")
        py_send("0,22,0")
        py_send("0,22,2")
        py_send("0,26,2")
        py_send("0,26,0")
        py_send("*add_elements")
        max_nodes_id = py_get_int("max_node_id()")
        py_send("%f,%f,%f,%f"           %           (max_nodes_id-1,max_nodes_id,max_nodes_id-
3,max_nodes_id-2))
        py_send("*set_duplicate_translations")
        py_send("0,%f,0" % (y_el))
        py_send("*set_duplicate_repetitions")
         nr_elem_breite2 = 11
        py_send("%f" % (nr_elem_breite2-1))
        py_send("*duplicate_elements")
        max_elements_id = py_get_int("max_element_id()")
        py_send("%f" % (max_elements_id))
        py_send("#")
        py_send("*sweep_nodes")
        py_send("all_existing")

        py_send("*add_nodes")
        py_send("0,%f,0" % ((nr_elem_breite2*y_el)+22))
        py_send("0,%f,2" % ((nr_elem_breite2*y_el)+22))
        py_send("0,%f,%f" % ((b/2),t))
        py_send("0,%f,0" % (b/2))
        py_send("*add_elements")
        max_nodes_id = py_get_int("max_node_id()")
        py_send("%f,%f,%f,%f"           %           (max_nodes_id-1,max_nodes_id,max_nodes_id-
3,max_nodes_id-2))
        py_send("*sweep_nodes")
        py_send("all_existing")

        py_send("*sub_divisions")
        py_send("3,2,3")
        py_send("*set_sweep_tolerance")
        py_send("0.1")
         py_send("*subdivide_elements")
        nr_nodes = py_get_int("nnodes()")
        nr_elements = py_get_int("nelements()")
        for i in range(1, nr_elements):
            zaehler = 0
            y_node = 0
                element_id = py_get_int("element_id(%i)" % i)
                for i in range(1, 4):
                  element_node_id = py_get_int("element_node_id(%f,%f)" % (element_id,i))
                  y_node = py_get_float("node_y(%i)" % element_node_id)
                if y_node <= (a+4) and y_node >= (a-4):
                                zaehler = zaehler + 1
            if zaehler > 0:
                        py_send("%i" % element_id)
        py_send("#")

        py_send("*add_points")
        py_send("0,%f,0" % (a-5))
        py_send("0,%f,%f" % ((a-5),t))
        py_send("0,%f,0" % (a+5))
        py_send("0,%f,%f" % ((a+5),t))

        py_send("*move_nodes_to_point")
```

```
py_send("1")
nr_elements = py_get_int("nelements()")
for i in range(1, nr_elements):
      element_id = py_get_int("element_id(%i)" % i)
           for i in range(1, 5):
            element_node_id = py_get_int("element_node_id(%f,%f)" % (element_id,i))
            y_node = py_get_float("node_y(%i)" % element_node_id)
            z_node = py_get_float("node_z(%i)" % element_node_id)
           if y_node <= (a-5+(t/2))+0.1 and y_node >= (a-5+(t/2))-0.1 and z_node == 0:
                            element_node_id = py_get_int("element_node_id(%f,%f)" %
(element_id,i))
                            py_send("%i" % element_node_id)

           if y_node == (a-5) and z_node >= 0.6 and z_node <= 0.7:
                            element_node_id = py_get_int("element_node_id(%f,%f)" %
(element_id,i))
                            py_send("%i" % element_node_id)
py_send("#")

py_send("*move_nodes_to_point")
 py_send("2")
 for i in range(1, nr_elements):
      element_id = py_get_int("element_id(%i)" % i)
           for i in range(1, 5):
            element_node_id = py_get_int("element_node_id(%f,%f)" % (element_id,i))
            y_node = py_get_float("node_y(%i)" % element_node_id)
            z_node = py_get_float("node_z(%i)" % element_node_id)
           if (y_node == (a-5+t/2) and z_node == t):
                            element_node_id = py_get_int("element_node_id(%f,%f)" %
(element_id,i))
                            py_send("%i" % element_node_id)

           if y_node == (a-5) and z_node >= 1.3 and z_node <= 1.4:
                            element_node_id = py_get_int("element_node_id(%f,%f)" %
(element_id,i))
                            py_send("%i" % element_node_id)
    py_send("#")

py_send("*move_nodes_to_point")
 py_send("3")
 nr_elements = py_get_int("nelements()")
for i in range(1, nr_elements):
      element_id = py_get_int("element_id(%i)" % i)
           for i in range(1, 5):
            element_node_id = py_get_int("element_node_id(%f,%f)" % (element_id,i))
            y_node = py_get_float("node_y(%i)" % element_node_id)
            z_node = py_get_float("node_z(%i)" % element_node_id)
           if (y_node == (a+5-t/2) and z_node == 0):
                            element_node_id = py_get_int("element_node_id(%f,%f)" %
(element_id,i))
                            py_send("%i" % element_node_id)

           if y_node == (a+5) and z_node >= 0.6 and z_node <= 0.7:
                            element_node_id = py_get_int("element_node_id(%f,%f)" %
(element_id,i))
                            py_send("%i" % element_node_id)
py_send("#")

py_send("*move_nodes_to_point")
 py_send("4")
```

```
 for i in range(1, nr_elements):
element_id = py_get_int("element_id(%i)" % i)
        for i in range(1, 5):
         element_node_id = py_get_int("element_node_id(%f,%f)" % (element_id,i))
         y_node = py_get_float("node_y(%i)" % element_node_id)
         z_node = py_get_float("node_z(%i)" % element_node_id)
        if (y_node == (a+5-t/2) and z_node == t):
                element_node_id = py_get_int("element_node_id(%f,%f)" % (element_id,i))
                py_send("%i" % element_node_id)

        if y_node == (a+5) and z_node >= 1.3 and z_node <= 1.4:
                element_node_id = py_get_int("element_node_id(%f,%f)" % (element_id,i))
                py_send("%i" % element_node_id)
py_send("#")

py_send("*sweep_nodes")
py_send("all_existing")

py_send("*add_nodes")
py_send("0,%f,0" % (b/2))
py_send("0,%f,%f" % (b/2,t))
py_send("0,%f,%f" % (b/2+t_f,t))
py_send("0,%f,0" % (b/2+t_f))
py_send("*add_elements")
max_nodes_id = py_get_int("max_node_id()")
py_send("%f,%f,%f,%f" % (max_nodes_id-1,max_nodes_id,max_nodes_id-3,max_nodes_id-2))

py_send("*add_nodes")
py_send("0,%f,0" % (b/2))
py_send("0,%f,0" % (b/2+t_f))
py_send("0,%f,%f" % (b/2+t_f,-2.8))
py_send("0,%f,%f" % (b/2,-2.8))
py_send("*add_elements")
max_nodes_id = py_get_int("max_node_id()")
py_send("%f,%f,%f,%f" % (max_nodes_id-1,max_nodes_id,max_nodes_id-3,max_nodes_id-2))

py_send("*set_duplicate_translations")
py_send("0,0,%f" % (-2.8))
py_send("*set_duplicate_repetitions")
py_send("4")
py_send("*duplicate_elements")
max_elements_id = py_get_int("max_element_id()")
py_send("%f" % max_elements_id)
py_send("#")

py_send("*add_nodes")
py_send("0,%f,%f" % (b/2,t))
py_send("0,%f,%f" % (b/2+t_f,t))
py_send("0,%f,%f" % (b/2+t_f,4.8))
py_send("0,%f,%f" % (b/2,4.8))
py_send("*add_elements")
max_nodes_id = py_get_int("max_node_id()")
py_send("%f,%f,%f,%f" % (max_nodes_id-1,max_nodes_id,max_nodes_id-3,max_nodes_id-2))

py_send("*set_duplicate_translations")
```

```
        py_send("0,0,%f" % (2.8))
        py_send("*set_duplicate_repetitions")
        py_send("4")
        py_send("*duplicate_elements")
        max_elements_id = py_get_int("max_element_id()")
        py_send("%f" % max_elements_id)
        py_send("#")

        py_send("*sweep_nodes")
        py_send("all_existing")

        py_send("*set_expand_translations")
         py_send("5,0,0")
        py_send("*expand_elements")
        py_send("all_existing")

        py_send("*sweep_nodes")
        py_send("all_existing")

        py_send("*set_duplicate_translations")
        py_send("5,0,0")
        py_send("*set_duplicate_repetitions")
        py_send("%f" % ((l/5)-1))
        py_send("*duplicate_elements")
        py_send("all_existing")
        py_send("#")

        py_send("*sweep_nodes")
        py_send("all_existing")


def main():

        global pi
        pi = 3.14159265
        e  = 2.718281828

        #  t             Dicke
        #  b             Breite mit Flanschdicke
        #  l             Länge
        #  t_f           Flanschdicke
        #  a             Abstand des Biegerarius von der Profilmitte im Querschnitt


        t = 2.0
        b = 136.4
        l = 1300.0
        t_f = 1.2

        b = b - 2*t_f

        ########################################

        modellAufbau(t,b,l,a,t_f)

        ########################################

if __name__ == '__main__':
        main()
```

CURRICULUM VITAE

Mehmet Okan Görtan was born in Kocaeli, Turkey in 1981. He finished Istanbul Erkek Lisesi in 2000. Afterwards, he earned his B.Sc. degree as a mechanical engineer from Istanbul Technical University in 2005. He started as a master’s student in Mechanical Engineering Department Design Program at the same university. After completing the coursework, he made his master studies at TU Darmstadt at PtU (Produktionstechnik und Umformmaschinen) in Germany.